



## Location of the photosynthetic carbon metabolism in microcompartments and separated phases in microalgal cells

Hélène Launay, Luisana Avilan, Cassy Gérard, Goetz Parsiegla, Véronique Receveur-brechot, Brigitte Gontero, Frédéric Carriere

### ► To cite this version:

Hélène Launay, Luisana Avilan, Cassy Gérard, Goetz Parsiegla, Véronique Receveur-brechot, et al.. Location of the photosynthetic carbon metabolism in microcompartments and separated phases in microalgal cells. FEBS Letters, 2023, 10.1002/1873-3468.14754 . hal-04290010

**HAL Id: hal-04290010**

**<https://hal.science/hal-04290010>**

Submitted on 16 Nov 2023

**HAL** is a multi-disciplinary open access archive for the deposit and dissemination of scientific research documents, whether they are published or not. The documents may come from teaching and research institutions in France or abroad, or from public or private research centers.


L'archive ouverte pluridisciplinaire **HAL**, est destinée au dépôt et à la diffusion de documents scientifiques de niveau recherche, publiés ou non, émanant des établissements d'enseignement et de recherche français ou étrangers, des laboratoires publics ou privés.



Distributed under a Creative Commons Attribution 4.0 International License

## PERSPECTIVE

# Location of the photosynthetic carbon metabolism in microcompartments and separated phases in microalgal cells

Hélène Launay , Luisana Avilan, Cassy Gérard, Goetz Parsieglia, Véronique Receveur-Brechot, Brigitte Gontero and Frédéric Carrière

Aix Marseille Univ, CNRS, BIP, UMR7281, Marseille, France

## Correspondence

H. Launay, Aix Marseille Univ, CNRS, BIP, UMR7281, F-13402 Marseille, France  
 Tel: +33491 16 41 92  
 E-mail: [helene.launay@univ-amu.fr](mailto:helene.launay@univ-amu.fr)

(Received 16 June 2023, revised 4 September 2023, accepted 22 September 2023)

doi:10.1002/1873-3468.14754

Edited by Peter Brzezinski

**Carbon acquisition, assimilation and storage in eukaryotic microalgae and cyanobacteria occur in multiple compartments that have been characterised by the location of the enzymes involved in these functions. These compartments can be delimited by bilayer membranes, such as the chloroplast, the lumen, the peroxisome, the mitochondria or monolayer membranes, such as lipid droplets or plasmoglobules. They can also originate from liquid–liquid phase separation such as the pyrenoid. Multiple exchanges exist between the intracellular microcompartments, and these are reviewed for the CO<sub>2</sub> concentration mechanism, the Calvin–Benson–Bassham cycle, the lipid metabolism and the cellular energetic balance. Progress in microscopy and spectroscopic methods opens new perspectives to characterise the molecular consequences of the location of the proteins involved, including intrinsically disordered proteins.**

**Keywords:** bioenergetics; Calvin–Benson–Bassham cycle; *Chlamydomonas reinhardtii*; cyanobacterium; diatom; intrinsically disordered protein; liquid–liquid phase separation; nuclear magnetic resonance; photosynthesis; structural biology

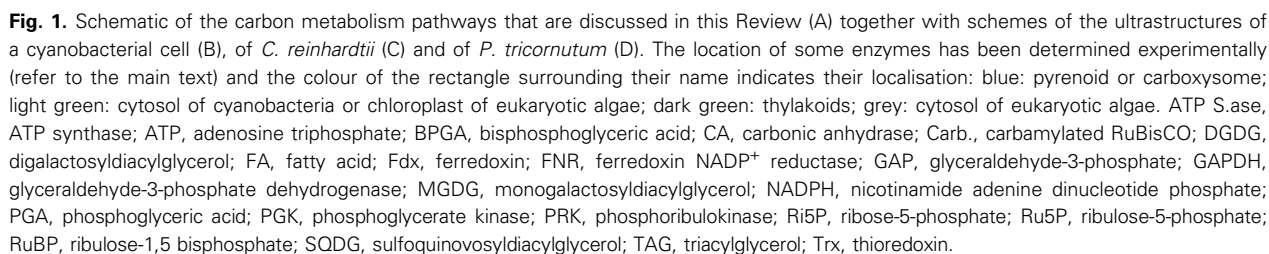
Photosynthesis is an essential metabolic pathway that allows autotrophic organisms to mobilise inorganic carbon and produce carbohydrates and fatty acids that

are further used by other metabolic pathways. These pathways are differentially localised in compartments that have distinct physicochemical properties, which

## Abbreviations

ALA,  $\alpha$ -linolenic acid; ARA, arachidonic acid; ATP S.ase, ATP synthase; ATP, adenosine triphosphate; BPGA, bisphosphoglyceric acid; CA, carbonic anhydrase; Carb., carbamylated; CBB, Calvin–Benson–Bassham; CCM, CO<sub>2</sub> concentration mechanism; CEF, cyclic electron flux; DAG, diacylglycerol; DES, deep eutectic solvents; DGAT, diacylglycerol acyltransferase; DGDG, digalactosyldiacylglycerol; DGTS, diacylglyceroltrimethylhomo-Ser; DHA, docosahexaenoic acid; EPA, eicosapentaenoic acid; EPYC1, essential pyrenoid component 1; ER, endoplasmic reticulum; FA, fatty acid; FAS, fatty acid synthase; FBPase, fructose-1,6 bisphosphatase; Fdx, ferredoxin; FNR, ferredoxin NADP<sup>+</sup> reductase; FRAP, fluorescence recovery after photobleaching; GAP, glyceraldehyde-3-phosphate; GAPDH, glyceraldehyde-3-phosphate dehydrogenase; IDP, intrinsically disordered protein; LD, lipid droplet; LEF, linear electron flux; LLPS, separated liquid–liquid phases; MGDG, monogalactosyldiacylglycerol; MLDP, major LD protein; NaDES, natural DES; NADPH, nicotinamide adenine dinucleotide phosphate; NMR, nuclear magnetic resonance; NTR, N-terminal repeat regions; OPP, oxidative pentose phosphates; PC, phosphatidylcholine; PDB, protein data bank; PG, phosphatidylglycerol; PGA, phosphoglyceric acid; PGD1, plastid galactoglycerolipid degradation 1; PGK, phosphoglycerate kinase; PRI, ribose-5-phosphate isomerase; PRK, phosphoribulokinase; PSI, photosystem I; PSII, photosystem II; PTM, post-translational modifications; PUFA, polyunsaturated fatty acids; Ri5P, ribose-5-phosphate; Ru5P, ribulose-5-phosphate; RuBisCO, Ribulose-1,5-bisphosphate carboxylase/oxygenase; RuBP, ribulose-1,5 bisphosphate; SAXS, small-angle X-ray scattering; SBPase, sedoheptulose-1,7 bisphosphatase; SQDG, sulfoquinovosyldiacylglycerol; SSUL, RuBisCO small subunit like domain; TAG, triacylglycerol; TPI, triose phosphate isomerase; Trx, thioredoxin.

acquisition of inorganic carbon and its accumulation at the location of the enzyme ribulose-1,5-bisphosphate carboxylase/oxygenase (RuBisCO; Fig. 1). In the



second stage, RuBisCO fixes CO<sub>2</sub> with a carboxylation step and produces two molecules of phosphoglyceric acid (PGA), a three-carbon molecule that is further converted into reduced carbohydrates in the Calvin–Benson–Bassham (CBB) pathway. The CBB pathway relies on the availability of a reducing power and adenosine triphosphate (ATP) generated by the photochemical phase of photosynthesis. Finally, the third stage is the synthesis of the carbon storage compounds in the form of either carbohydrates or fatty acids further esterified into membrane and storage lipids (triacylglycerol lipids). Each of these three stages is finely tuned according to light intensity, availability of the inorganic carbon source or environmental stresses (nutrient shortage, temperature, salinity, drought, pressure, etc.).

The molecular mechanisms underlying the regulation of carbon acquisition, assimilation and storage pathways are well-described in the literature. These involve physicochemical transitions such as changes in pH, redox potential, metabolites and metal ion concentrations within the cellular compartments where photosynthesis occurs [1–4], post-translational modifications [5–7], structural transitions of key enzymes [8–10] and reorganisations within supramolecular complexes [11–14]. Recent high-resolution cryo-electron microscopy images and tomograms from the cyanobacterium *Synechocystis* 6803 [15], the green alga *Chlamydomonas reinhardtii* [16–18] and the diatom *Phaeodactylum tri-cornutum* [19] enabled the cellular localisation of some metabolic pathways. The location of enzymes within the cells (Fig. 1B) can be correlated with the molecular description of the biochemical pathways (Fig. 1A) thanks to progress in biophysical methods such as microscopy, mass spectrometry, several spectroscopic methods such as fluorescence spectroscopy and nuclear magnetic resonance (NMR) and machine-learning-assisted-data interpretation [16,20,21].

Here, we will focus on unicellular photosynthetic organisms, where all stages of the carbon cycle occur in a single cell, unlike most higher plants. In multicellular organisms, cell specialisation can allow to separate physiological functions on the macroscopic level. In eukaryotic unicellular photosynthetic organisms, different organelles participate in the compartmentalisation of some metabolic pathways. This partitioning helps prevent futile cycles of antagonist metabolic pathways that share the same metabolites. For example, the oxidative pentose phosphate (OPP) cycle in diatoms is localised in the cytoplasm, and its antagonist pathway, the CBB, also named reductive pentose phosphate cycle, is localised in the chloroplast [22]. In eukaryotic microalgae, inorganic carbon is imported

and assimilated in the chloroplasts (Fig. 1B). Carbon storage is then ensured by the synthesis of polysaccharides that accumulate in the form of starch granules in the chloroplast of green algae, of starch-like polymers in cyanobacteria [23], or of chrysolaminarin granules in the vacuoles of diatoms [24,25]. Alternatively, carbon can be stored through the synthesis of triacylglycerols (TAG) that assemble in lipid droplets (LD) [26]. Even though these carbon metabolic pathways are separated in different spaces within the cell, they are interconnected by exchange of metabolites between the different partitions and across their boundaries.

The physical–chemical nature of these cell compartments varies. For example, LDs encapsulate an organic liquid phase [27], whereas polysaccharide granules are composed of amorphous and semicrystalline layers of polysaccharides [27–29]. Traditionally, the term ‘organelle’ refers to large aqueous cellular compartments surrounded by a bilayer membrane such as the chloroplast, the vacuole or the mitochondrion. The term organelle has been also proposed to name LDs that are smaller organic partitions surrounded by a monolayer membrane [27,30]. Organelles can be themselves divided in different regions of space that we chose to name microcompartments. For example, polysaccharide granules that localise within the chloroplast of green microalgae or within the vacuole of diatoms can be referred to as a microcompartment. One can also refer to the self-assembled granules of polysaccharide as ‘biomolecular condensates’. Indeed, the term ‘condensation’ has been used to denominate the spontaneous clustering of biomolecules that result in a high local concentration surrounded by a dilute phase and the partitioning of the cell [31]. Different types of biomolecules can spontaneously cluster in biomolecular condensates, including ribonucleic acid, polysaccharides, proteins or lipids [32–34]. The pyrenoid matrix is a well-described example of protein biomolecular condensate that is described in details in [Pyrenoid and carboxysome](#) section. Because biomolecular condensates do not possess membranes, they are also referred to as membrane-less organelles [32–34]. The physicochemical properties of these biomolecular condensates are the focus of intense scrutiny.

Microcompartments can be observed in microscopy images of prokaryotic unicellular organisms, such as carboxysomes, in nonheterocystous cyanobacteria, where inorganic carbon and RuBisCO are condensed [35]. The thylakoid membranes can also be considered as a microcompartment because they define a new region of space in the chloroplast where the photochemical phase of photosynthesis produces ATP and NADPH. Their associated plastoglobules are another

example of partition, the function of which is multiple [36]. Plastoglobules encapsulate a hydrophobic core with varying compounds that change according to culture conditions, surrounded by a monolayer membrane [37]. They have been proposed to provide storage for thylakoid components, and to be involved in insoluble isoprenoid synthesis or degradation, and in stress response, as well as in the storage of compounds that can be toxic for the cell such as terpenes [36,38].

This perspective review aims to discuss the organisation of carbon metabolism in different microcompartments and at different scales within the cell. This includes the molecular description of the regulatory processes with the physical separation of their key actors, as well as the formation of supramolecular assemblies/biocondensates leading to the segregation of metabolites and enzymes.

### Illustration from the emblematic case of RuBisCO

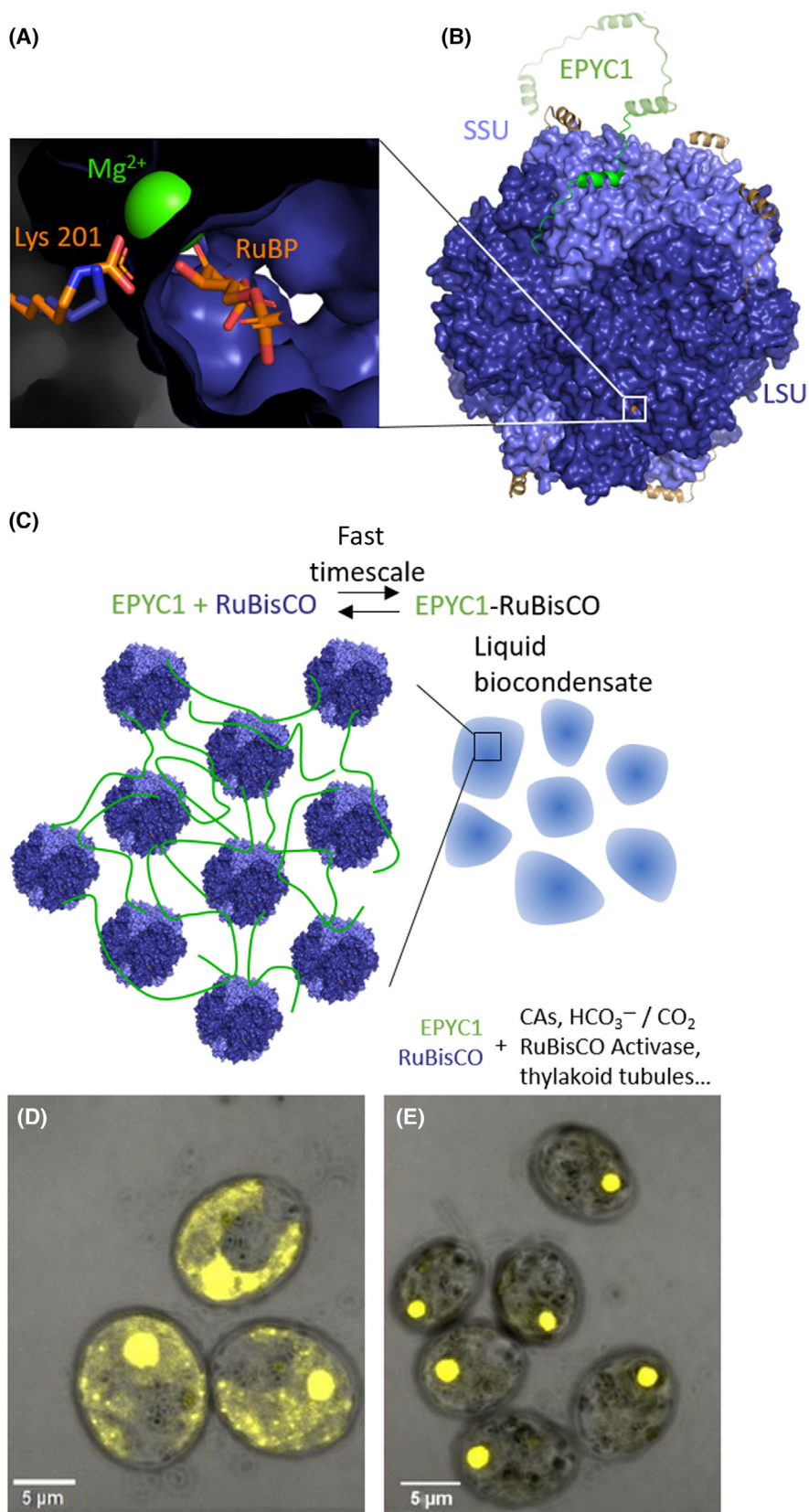
The study of RuBisCO, which is a complex made up of large (L) and small (S) subunits (Fig. 2A), is emblematic of the structure–function relationships in a complex [39]. Since the first X-ray structure of the active RuBisCO in 1989 [40], more than 240 structures from all the photosynthetic lineage have been deposited in the Protein Data Bank (PDB). The mainly described oligomeric state of the enzyme is the L<sub>8</sub>S<sub>8</sub> hexadecameric form, but other oligomeric states exist [41]. The regulation of the enzyme, notably by pH, a Mg<sup>2+</sup> cation and an ‘activating’ nonsubstrate CO<sub>2</sub> molecule via the carbamylation of Lysine 201 in the active site of the large subunit is well-understood [7] (numbering from *C. reinhardtii*, Fig. 2A). Binding of RuBP to noncarbamylated RuBisCO results in an inhibited state. This state is resolved by interaction with a RuBisCO activase or possibly by CBB X protein (CbbX) in diatoms [42,43]. The ‘structure–function’ correlation of this model enzyme is thus well-established. Since more than 30 years, its localisation in an ultrastructure has been observed on microscopy images: in the pyrenoid in eukaryotic microalgae

or in the carboxysomes in cyanobacteria [35,44–46]. More precisely, in *C. reinhardtii* and under atmospheric CO<sub>2</sub> (~400 ppm) and O<sub>2</sub> concentrations, RuBisCO is present both in the chloroplast stroma and in the pyrenoid microcompartment (Fig. 2D). Under CO<sub>2</sub> concentrations lower than atmospheric (<200 ppm) or high O<sub>2</sub> conditions, RuBisCO relocates from the stroma to the pyrenoid (Fig. 2E) [18,47,48]. Only very recently, the physicochemical nature of the pyrenoid has been described. This biomolecular condensate is detailed in the following section [32,49–52]. Also, recent metabolic flux models provide insights into the consequence of this ‘segregation’ or ‘condensation’ of RuBisCO within these demixing condensates as regard to the CBB metabolic flux [18].

From the example of RuBisCO, one can now extend the ‘structure–function’ relationships from quaternary structure (oligomeric enzyme complex) to an additional level of supramolecular assembly that could be named ‘ultrastructure–function’ relationships. Such an organisation raises new questions. What is the significance of the heterogeneity within a cell, in other words ‘roughness’, observed in microscopy images [53,54]? What are the physicochemical properties of the various microcompartments? Some are mesoscopic macromolecular complexes such as carboxysomes or starch granules. Some are separated liquid phases that demix because of the presence of different water-insoluble compounds such as lipids. Some are separated liquid phases that demix because of condensation of protein constituents through multivalent transient intermolecular interactions such as the pyrenoid [33,34,55]. While the phase separation of lipids appears obvious, why do carbohydrates (starch) and proteins (pyrenoid) also phase separate? These microcompartments cannot be considered as strictly confined zones, as metabolites diffuse in and out. How is their formation/disassembly regulated? How do proteins fold in these different microcompartments? All these questions can be raised for each stage of the carbon cycle of microalgae, but this is also true for all metabolic pathways in all types of cells.

**Fig. 2.** RuBisCO regulation at the molecular and supramolecular levels. (A) Structure of the active site of RuBisCO (PDB ID: 1IR2). (B) Hexadecameric L<sub>8</sub>S<sub>8</sub> RuBisCO bound to eight Essential Pyrenoid Component 1 (EPYC1) proteins, obtained by cocrystallisation with saturating concentrations of synthetic peptides shown in brown (PDB IDs: 7JSX and 7JFO). In addition, one full-length EPYC1 protein is artistically depicted in green. (C) Schematic of the molecular contacts between EPYC1 and RuBisCO underlying the phase separation. (D, E) Confocal microscopy images of *C. reinhardtii* showing Venus-labelled RuBisCO that indicating the location of the hexadecameric complex. (D) Location of RuBisCO in both the chloroplast stroma and the pyrenoid at atmospheric CO<sub>2</sub> concentration with 5 mM bicarbonate. (E) Hyperoxia phenotype and the relocation of RuBisCO induced by 100 μM H<sub>2</sub>O<sub>2</sub> to the culture. Panels D and E are adapted from [48]. The same relocation is observed under low CO<sub>2</sub> conditions without hyperoxia.





Ideally, to grasp the above-defined ‘ultrastructure-function’ relationships, one would like to be able to describe all the ultrastructural elements observed on electron microscopy images at the molecular level and provide a rationale on their role for the regulation of the metabolic pathways they are hosting. Most of the recent technological developments that allowed deciphering some of these aspects on the carbon metabolism of microalgae will be mentioned.

## Pyrenoid and carboxysome

As mentioned above, the most emblematic enzyme for CO<sub>2</sub> fixation is RuBisCO, which is responsible for the conversion of 10<sup>14</sup> kilogrammes of carbon each year [56]. Surprisingly, the maximum catalytic activity for the carboxylation of RuBP by RuBisCO is achieved at significantly high CO<sub>2</sub> concentrations (ranging from 25 to 100 µM). These concentrations are higher than the atmospheric CO<sub>2</sub> concentration (c.a. 15 µM in the oceans) [57,58]. The pH of the compartment where RuBisCO is localised, such as the chloroplast stroma or the cyanobacteria cytosol (pH 7.9), suggests that the major form of inorganic carbon is bicarbonate. Considering these biochemical data, it can be concluded that RuBisCO is not working at its maximum rate and that the carboxylation reaction is in competition with the oxygenation of RuBP. The latter produces an inhibitor of the CBB cycle, 2-phosphoglycolate, that must be metabolised in the C2 respiratory pathway. This apparent paradox may be resolved when the ultrastructure of the chloroplast is taken into consideration. The chloroplast membranes, including the thylakoids membranes, are permeable to CO<sub>2</sub>, and bicarbonate transporters catalyse the import of HCO<sub>3</sub><sup>−</sup> into the stroma (Fig. 1B). In each compartment, carbonic anhydrases catalyse the HCO<sub>3</sub><sup>−</sup>/CO<sub>2</sub> conversion so that their pH-dependent ratio is instantly achieved. Besides, the equilibrium across multiple microcompartments that have different pH—the thylakoids lumen (pH 6) versus the chloroplast stroma and the pyrenoid (pH 7.9)—drives the import of inorganic carbon to the pyrenoid [57]. The ‘passive’ transport of inorganic carbon through the different microcompartments can support RuBisCO carboxylation activity in the pyrenoid under atmospheric CO<sub>2</sub> conditions, while additional HCO<sub>3</sub><sup>−</sup> transporters enhance inorganic carbon import under low CO<sub>2</sub> [59]. Finally, the condensation of RuBisCO together with CAs in the carboxysome (cyanobacteria) or the pyrenoid (eukaryotic microalgae) increases the availability of CO<sub>2</sub> in the vicinity of the enzyme, which enables its activity. The pyrenoid is often surrounded by a discontinuous layer of starch granules that could contribute to the confinement of

inorganic carbon that results in a higher CO<sub>2</sub>/O<sub>2</sub> ratio compared with the stroma and that supports carboxylation at the expense of oxygenation reaction [47]. Under specific conditions (hyperoxia), the pyrenoid has no starch sheath and presents a large interface with the chloroplast stroma [48]. The existence of such interface will be discussed later.

For decades, it was enigmatic how the colocalisation of RuBisCO and CAs was mediated, even though the functions of the carboxysome and pyrenoid were known [35,44,45]. RuBisCO was copurified in cyanobacterial β-carboxysome as a supramolecular complex with small putative shell proteins (CcmM) that are composed of three RuBisCO small subunit-like domains (SSUL) and one isoform that possesses a CA domain [60]. Reconstitution of the RuBisCO–CcmM complexes *in vitro* induced a liquid–liquid phase separation: One phase is a biomolecular condensate of RuBisCO–CcmM and the other phase is free of proteins [61,62]. In a nutshell, multivalent interactions between the hexadecameric RuBisCO (L<sub>8</sub>S<sub>8</sub>) and the SSUL domains result in the condensation of the two protein complexes when they are mixed in the appropriate stoichiometry (0.25 : 1 molar ratio). The reversible demixing of these two separated liquid–liquid phases (LLPS) can be observed using fluorescent-tagged proteins and fluorescence microscopy. Demixing does not occur under high salt concentrations that interfere with electrostatic intermolecular interactions. Also excess of CcmM prevented the condensation of the separated liquid phase, indicating that stoichiometry is essential [61]. The fluidic (liquid) nature of the protein condensate was confirmed by dual-colour fluorescence cross-correlation spectroscopy and fluorescence recovery after photobleaching (FRAP) that allowed to quantify the short live-time of the RuBisCO–CcmM contacts.

Similarly, the α-carboxysome biogenesis involves multivalent interactions of the hexadecameric RuBisCO with four N-terminal repeat regions (NTR) of a large (~ 900 residues) intrinsically disordered protein (IDP) named CsoS2. Demixing into two liquid–liquid phases was observed when RuBisCO and CsoS2–NTR are present in the appropriate stoichiometry (1 : 1 molar ratio) [63]. The dynamics that are characteristic for the LLPS biocondensates only have been studied by *in vitro* studies of carboxysomes biogenesis. This biphasic state is not conserved in the final mesoscopic RuBisCO–CA supramolecular complex, that is surrounded by shell proteins. This suggests that the transient interactions are fixed upon the recruitment of other partners of the final aggregates that acquire microcrystalline properties [64].

Unlike carboxysomes, the pyrenoid has no protein-shell. It has been a challenge to isolate this membrane-less microcompartment in order to identify its molecular constituents. It is not a microcrystalline structure and therefore it loses its integrity upon purification steps. The constituents of the pyrenoid were identified by a combination of genetic screening with the creation of a library of GFP-mutant chloroplast proteins, microscopy and proteomic screening [65]. An essential protein for the formation of the pyrenoid is the Essential Pyrenoid Component 1 (EPYC1) that has no enzymatic activity [66]. Like CsoS2, EPYC1 (in *C. reinhardtii*) is an IDP composed of five repeat domains having a small RuBisCO subunit binding site (Fig. 2B). If EPYC1 and hexadecameric RuBisCO are present in a defined stoichiometry (2 : 1 molar ratio), demixing into two phases occurs in a process similar to that of the RuBisCO : CcmM or the RuBisCO : CsoS2 biomolecular condensates [49,51]. As for the RuBisCO–CcmM biocondensates, the demixing is prevented by high salt concentration or by excess of EPYC1 or RuBisCO, indicating that the multivalent electrostatic interactions are essential for the condensation. Similarly, FRAP revealed the very transient EPYC1 : RuBisCO contacts, which is also a hallmark for LLPS and the formation of biocondensates [51] (Fig. 2C).

EPYC1, CsoS2 or CcmM act as scaffolds, ‘smooth mortar’ or ‘stickers’ to confine RuBisCO in a biomolecular condensate due to their multivalent binding sites with this enzyme. This condensate can maintain a high degree of freedom—liquid properties—because the intermolecular interactions are transient. Other factors can contribute to the rigidification as it is the case for the mature carboxysomes. On the contrary, in the cells, the pyrenoid retains a high degree of freedom that characterises liquid droplets. The absence of a stable three-dimensional structure in CsoS2 and EPYC provides an extra level of flexibility to the scaffold. Intrinsically disordered proteins are described as essential in the responsiveness to stimuli, and their roles in the regulatory network also have been demonstrated for the regulation of the carbon metabolism [11]. Their structural flexibility enables fast re-arrangement upon exposition to different conditions, such that they can act as sensors. For example, the intrinsically disordered region of the MAPK phosphatase AP2C3 of *Arabidopsis thaliana* was proposed to be the CO<sub>2</sub> sensor that regulates the phosphatase activity in response to increasing CO<sub>2</sub> concentration [67]. The molecular description of AP2C3 revealed that the IDP fosters the condensation of LLPS droplets at 10 000 ppm CO<sub>2</sub>,

whilst the proteins were scattered or dispersed at atmospheric CO<sub>2</sub> concentrations (400 ppm). To our knowledge, the catalytic properties of RuBisCO in the pyrenoid compared with that free in solution is not known but new properties might emerge in this more complex environment. How the condensation of protein-dense phases might contribute to the catalytic efficiency will be discussed at the end of this perspective paper. Intrinsically disordered proteins are also prone to have post-translational modifications (PTMs) as response to signalling pathways, and these PTMs can trigger dissociation of LLPS as it is the case for histone containing LLPS [68]. Altogether, IDPs are considered as key regulators for the formation/dissassembly of LLPS [69].

Intrinsically disordered proteins are also often described as ‘hub’ proteins, a property observed for several scaffold proteins in liquid biomolecular condensates. The full molecular properties of EPYC or CsoS2 in the condensates are not yet described. Only transient contacts between the scaffold protein and RuBisCO have been described by using fusion proteins with small polypeptides (Fig. 2B) [49,63]. It is expected that the entire proteins will remain highly flexible like other IDPs scaffolds for LLPS biocondensates. Several of them have been investigated at the residue-scale using NMR such as FUS [70], hnRNPA2 [71], CAPRIN1 [72,73], HP1 $\alpha$  [74], tau [75,76], Ntail [77] and TCP42 [78] (for global review, refer to [70]). Nuclear magnetic resonance can indeed complement the fluorescence-based methods that have mostly been employed to characterise the RuBisCO-containing LLPS. The NMR chemical shift reflects the structural properties of the protein at the residue-specific scale (are they in folded regions or disordered?). Putative conformational dynamic timescales can be probed using a range of NMR experiments (ns– $\mu$ s using spin relaxation experiments, 100  $\mu$ s–100 ms using relaxation dispersion or off-field saturation experiments) and the short-range and long-range transient contacts can be probed using nuclear Overhauser effect spectroscopy or paramagnetic relaxation enhancement experiments. A review of the recent NMR method developments and their use in structural biology can be found in Thiell et al. and Luchinat, Prog. in NMR Spec. (2022) [79]. In addition, recent developments of pulsed-field gradient NMR spectroscopy (or diffusion-ordered spectroscopy) can be used to discriminate the localisation of the proteins within the different phases [73,76]. Nuclear magnetic resonance is thus a unique method that can combine structural and physicochemical information in complex environments such as LLPS.



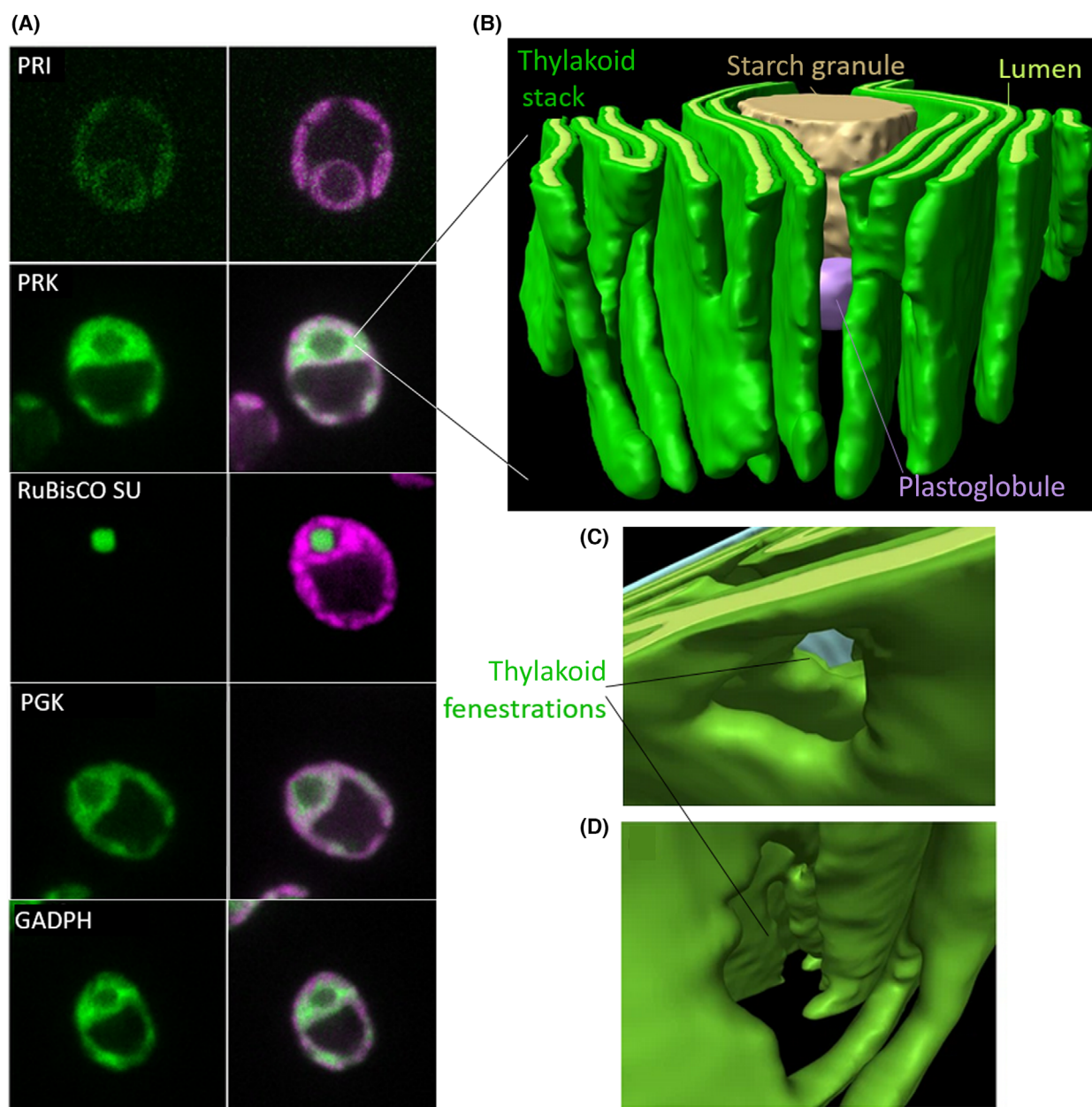
## Regulation of the RuBisCO substrate regeneration

The positive effect of pyrenoid or carboxysome formation for the availability of CO<sub>2</sub> in the vicinity of the RuBisCO active site has been modelled [18,57], but their effect for the availability of the sugar substrate, RuBP, within these microcompartments is puzzling. In the higher plant *Nicotiana tabacum*, the RuBP carboxylation by RuBisCO is not the rate limiting step for CO<sub>2</sub> assimilation, but the RuBP regeneration by the CBB enzymes is limiting [80], and one could assume that it is the same in green microalgae. The last step of RuBP regeneration is performed by the phosphoribulokinase (PRK) that catalyses the phosphorylation of ribulose-5-phosphate with ATP. Decrease of up to 80% of the amount of PRK did not affect CO<sub>2</sub> assimilation in *Nicotiana tabacum* and *C. reinhardtii*, indicating that the rate limiting step is not the last step of the RuBP regeneration [81,82]. Genetic engineering of a fluorescent-tagged protein library in *C. reinhardtii* allowed to localise PRK in the chloroplast stroma around the pyrenoid (Fig. 3A) [16,18], which raises the question of how the PRK product, RuBP, crosses the pyrenoid boundaries. Similarly, phosphoglycerate kinase (PGK) that catalyses the phosphorylation of RuBisCO product PGA into bisphosphoglycerate is also localised in the chloroplast stroma, such that the PGA has to migrate out of the pyrenoid. The bisphosphoglycerate is in turn reduced by the glyceraldehyde 3-phosphate dehydrogenase (GAPDH) that shares the same stromal localisation (Fig. 3A). It is known that substrate and cofactor availability is a key parameter in the regulation of the enzymes in general and of the CBB pathway in particular [1,83]: PRK and PGK phosphorylate their substrate by using ATP, and the reducing power of GAPDH is provided by NADPH. The availability of ATP and NADPH, both products of the photochemical stage that occurs on thylakoid membranes, is discussed below. In the cyanobacterium *Synechocystis pcc6803*, several CBB enzymes were localised by immunogold labelling and electron microscopy in proximity with the thylakoid membranes: 72% of the PRK particles, together with 66% of PGK and GAPDH and 47% of the observed RuBisCO particles [15].

Regulation of PRK is another emblematic case for the structure–function relationships. Since 2019, the crystal structure of the active PRK dimer is available as well as that of inactive PRK in supramolecular complexes with GAPDH and the small regulatory protein CP12 [9,84–86] (Fig. 4B). CP12 colocalises with PRK and GAPDH in the chloroplast stroma at the

periphery of the pyrenoid [16]. Activity assays of purified PRK revealed that it is regulated by its redox state: The reduction in inactive oxidised PRK is catalysed by thioredoxin f or m [87–89]. Phosphoribulokinase is thus a target of the ferredoxin–thioredoxin network as several other CBB enzymes [5]. The nature of the spatial organisation of the thylakoid membranes discussed below could be considered in this regulation. The molecular description of thioredoxin-mediated regulation of PRK was deciphered by a combination of mutagenesis, activity assays and crystallographic structures and can be summarised as follows. In its reduced state, the active site is localised in a groove that harbours Arg64 (numbering from the model *C. reinhardtii*) that can coordinate Ru5P and Cys16 that binds ATP (Fig. 4A) [9,90]. Upon oxidation, the disulphide-bond formation between Cys16 and Cys55 reorganises the ATP binding site (Fig. 4B). When oxidative conditions prevail, PRK has a high affinity for the GAPDH-CP12 subcomplex [91,92]. The N-terminal hairpin of CP12 that harbours the disulphide-bond Cys23–Cys31 occupies the active site groove of PRK [84,85]. The formation of the ternary complex is mediated by the redox-dependent structural transition of CP12 that we have described using NMR and small-angle X-ray scattering (SAXS) experiments: It is intrinsically disordered in reducing conditions and becomes partially ordered in oxidising conditions [12,93]. This protein is thus conditionally disordered and is a hub for the ternary complex association. The weak electron density observed for CP12 in the cryo-electron microscopy of the GAPDH-CP12-PRK complex suggests that it retains a high degree of flexibility within the ternary complex [84]. Interestingly, reduction and re-activation of PRK occurs faster when it is sequestered within the ternary complex compared with free oxidised PRK, and this is an example of how supramolecular organisation modifies the regulation [14,88,92,94]. Also, in the complex, PRK and GAPDH are protected from oxidative damage [95]. This large assembly also recruits another CBB enzyme: the aldolase, conferring new properties to this enzyme when embedded in this supramolecular edifice [96].

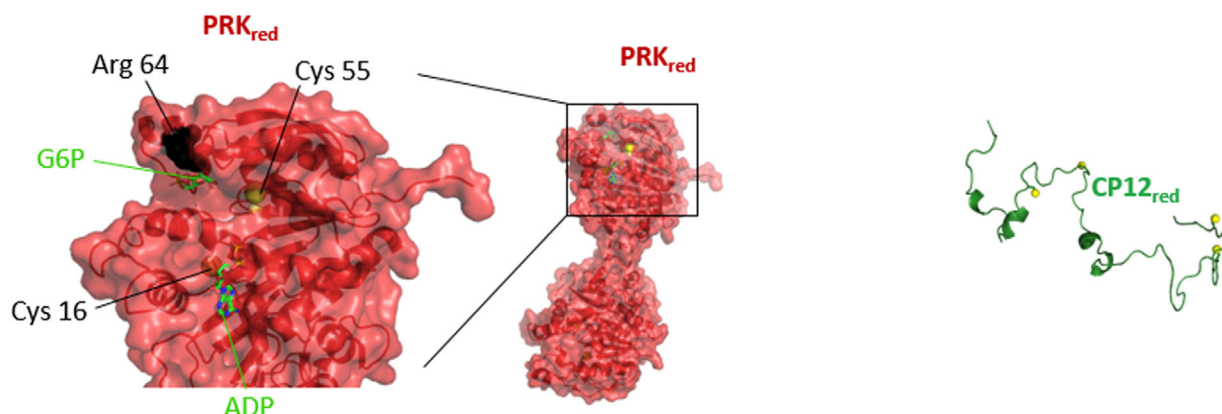
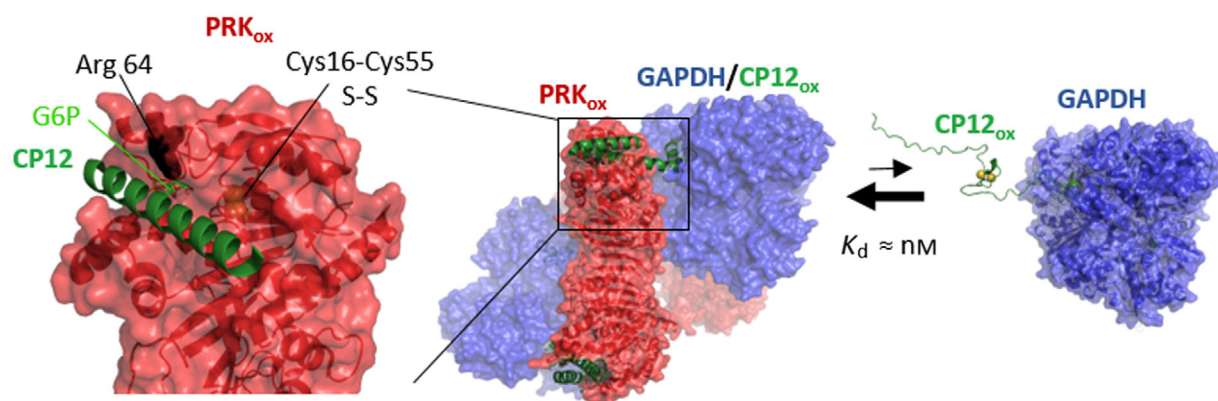
The recent molecular description of the GAPDH-CP12-PRK complex can be confronted to 30-year-old reports of copurification of active proteins (Table 1) [12]. For example in spinach, GAPDH and PRK were shown to associate with phosphoribose isomerase (PRI), RuBisCO, sedoheptulose-1,7-bisphosphatase and ferredoxin-NADP<sup>+</sup> reductase close to the thylakoid membranes [97]. Other studies revealed the association of at least PRI, PRK and RuBisCO in spinach [13], rice [98], tobacco [99], all



**Fig. 3.** (A) Location of different enzymes of the CBB cycle revealed by fluorescence microscopy using Venus-fusion constructs shown ingreen. The autofluorescence of chlorophyll is shown in purple. Figure adapted from [18]. (B) 3D organisation of the thylakoids stacks that shows the three continuous phases: the lumen (light green), the bilayer membrane (dark green) and the stroma. (C, D) Show fenestrations through the thylakoids that enable communications between different stroma compartments delimited by the thylakoids. Figure adapted from [17].

higher plants that are devoid of pyrenoids. The colocalisation of successive enzymes for the RuBP regeneration is a strategy to increase metabolite turnover [100]. In *C. reinhardtii* and other microalgae, however, PRI and PRK were not observed in the pyrenoid or carboxysomes. Nonetheless, RuBisCO is not sequestered in the pyrenoid or carboxysome under atmospheric or

high CO<sub>2</sub> conditions and therefore could be available for such supramolecular complexes (Fig. 2D) [15,48]. Despite the tremendous efforts that enable to solve the structure of homomeric complexes for most enzymes of the CBB cycle [1], no other supramolecular complexes except GAPDH-CP12-PRK or the transient complex of RuBisCO-EPYC1 have been reconstituted

(A) Light,  $E'_0 < -350$  mV(B) Dark,  $E'_0 > -350$  mV

**Fig. 4.** Regulation of PRK from the molecular to the supramolecular level: from left to right are shown the structure of the active site of PRK from *C. reinhardtii* in reducing conditions (PDB ID: 6H7G) and from *A. thaliana* in oxidising conditions (PDB ID: 6KEZ). The positions of the ATP/ADP and substrate are modelled thanks to alignment with the structure of *S. elongatus* PRK (PDB ID: 6KEV). In this structure PRK is crystallised with glucose-6-phosphate that can occupy the active site at the position of Ru5P. The Arg64 position is indicated. (A) In the light, reducing conditions prevails in the chloroplast stroma as it is indicated by the low Nernst potential ( $E'_0$ ). CP12 is intrinsically disordered [204] and the regulatory PRK disulphide Cys16-Cys55 bond is disrupted. (B) In the dark, oxidative conditions prevails in the chloroplast stroma as it is indicated by the higher Nernst potential. CP12 is partially folded, has a high affinity for GAPDH and the GAPDH-CP12 sub-complex in turn has a high affinity for PRK [205].

and studied *in vitro* (let aside the carboxysomes). Both of these complexes involve a hub or scaffold IDP, that has no enzymatic function: EPYC1 or CP12. The identification of CP12 was enabled decades ago thanks to its homology with the C-terminal extension of the B-isoform of GAPDH of higher plants [101]. The RuBisCO-EPYC1 interactions are transient and would not support copurification by classic chromatographic strategies, and it has thus escaped knowledge until recent proteomic studies [66]. The recent advances of mass spectrometry coupled with cross-linking agents could be in future at the origin of the identification of transient protein-protein interactions and of other

protein hubs that may mediate the association of other CBB enzymes in supramolecular complexes [102].

### ATP and reducing power generation

The acquisition of one CO<sub>2</sub> molecule (i.e. its transport to the vicinity of RuBisCO in the pyrenoid) consumes 1.3 ATP molecules [57], and its assimilation by the CBB cycle consumes two NADPH and three ATP molecules [1]. Their primary generation occurs in the thylakoid membranes via the proton gradient and the linear electron flux (LEF) that are generated on the photochemical phase of photosynthesis. This



**Table 1.** Supramolecular complexes containing CBB enzymes, the organism in which they have been observed and the related reference that had reported these complexes. CA, carbonic anhydrase; FBpase, fructose-1,6 bisphosphatase; FNR, ferredoxin NADP<sup>+</sup> reductase; GAPDH, glyceraldehyde-3-phosphate-dehydrogenase; PGK, phosphoglycerate kinase; PRI, ribose-5-phosphate isomerase; PRK, phosphoribulokinase; RuBisCO, ribulose-1,5 bisphosphate carboxylase/oxygenase; SBpase, sedoheptulose-1,7 bisphosphatase; TPI, triose phosphate isomerase.

Protein content	Organism	References
CA/PRK/RuBisCO/PGK	<i>Pisum sativum</i>	[188]
PRI/PRK/RuBisCO	<i>P. sativum</i>	[189]
PRI/PRK/RuBisCO/PGK	<i>P. sativum</i>	[190]
PRI/PRK/RuBisCO/PGK/GAPDH	<i>Spinacia oleracea</i>	[13]
	<i>Anacystis nidulans</i>	[191]
PRI/PRK/RuBisCO/PGH/GAPDH/ATP synthase	<i>Synechocystis 6803</i>	[15]
RuBisCO/PGK/GAPDH/TPI/aldolase/FBPase	<i>S. oleracea</i>	[192]
PRI/PRK/RuBisCO/PGH/GAPDH/SBPase/FNR/ATP synthase	<i>S. oleracea</i>	[193]
RuBisCO/PGK/GAPDH/TPI/aldolase/FBPase	<i>S. oleracea</i>	[192]
GAPDH/TPI/aldolase/SBPase	<i>P. sativum</i>	[190]
GAPDH/CP12/PRK	<i>S. oleracea</i>	[101,194,195]
	<i>P. sativum</i>	[194,195]
	<i>A. thaliana</i>	[196]
	<i>Galderia sulfuraria</i>	[197]
	<i>Synechocystis 6803</i>	[198,199]
	<i>Synechococcus PCC7942</i>	[200]
	<i>C. reinhardtii</i>	[199,201,202]
GAPDH/CP12/FNR complex	<i>Asterionella formosa</i>	[203]

photochemical process produces two NADPH and 2.6 ATP molecules, and the ATP : NADPH ratio is modulated by the Mehler reaction, the flavodiiron proteins and the cyclic electron flux (CEF) though their quantitative contribution is difficult to assess [103,104]. Malate valves that are discussed in the next section are also involved [105]. Before expending on the energetic balance across organelles in the case of eukaryotic algae, the supramolecular organisation of the thylakoid membranes (that is shared by prokaryote and eukaryote algae) is discussed. The thylakoids are bilayer membranes of amphiphilic lipids that adopt a well-organised structure that encapsulates a single internal aqueous phase that is the lumen, where protons accumulate from water splitting at the interface of photosystem II (PSII). This proton gradient force provides the energy for the ATP synthase to regenerate ATP. The electrons released from water splitting are transported by the quinone pool to the cytochrome *b<sub>6</sub>/f* and the photosystem I (PSI), and finally to ferredoxin and ferredoxin NADP<sup>+</sup> reductase (FNR). This LEF occurs between spatially separated photosystems: PSII accumulates in thylakoids stacks or grana that are multilayer packing of thylakoids, Cyt *b<sub>6</sub>/f* is more evenly distributed, whereas PSI accumulates in unstacked thylakoids lamellae together with ATP synthase [106]. It should be noted that in *C. reinhardtii*, the proportion of stacked over unstacked thylakoid membranes is much lower than that in higher plant, and the above-mentioned distribution can be balanced

[17,107]. Continuous progress of tomographic and cryo-electron microscopy will improve to decipher the localisation of the photosystem constituents [17]. The organic interface of the bilayer membranes and the lumen are continuous phases all through the chloroplast, such that there is a unique boundary between the lumen and the stroma and a unique thermodynamic balance between the two aqueous phases. The thylakoid lamellae where NADPH and ATP are regenerated separate the chloroplast stroma in a series of microcompartments; in other words, they create boundaries within the chloroplast stroma [53]. How do NADPH and ATP distribute through the chloroplast stroma under these circumstances? The recent electron microscopy tomograms of *C. reinhardtii* cells revealed that the thylakoids are pierced by fenestrations (Fig. 3B) that enable the different microcompartments of the stroma to communicate. As a consequence, the stroma is also a continuous tangled phase in which proteins and metabolites can diffuse. The heterogeneity and complex 3D boundaries render molecular motions highly complex in the stroma, and these effects on protein and metabolites are discussed in the last paragraph of the manuscript.

## Biosynthesis of thylakoid lipids and their supramolecular assembly

The thylakoid membranes should not be seen as rigid boundary, their assembly in bilayer membranes is

dictated by phase separation and this is highly dependent on temperature stress [108,109]. Furthermore, several molecular mechanisms involved in membrane-remodelling have been discovered, and the role of the lipid polar head and fatty acyl chain composition will be discussed below [110–113]. Membrane-associated protein can also play a role in membrane remodelling. For example, the molecular mechanism by which the protomers of IM30 protein (for Inner Membrane protein of 30 kDa) self-assemble to thylakoid membranes has been described using a range of biophysical techniques such as atomic-force spectroscopy, SAXS and modelling [114]. Their association with the thylakoids results in the formation of a protective carpet and their intrinsically disordered C-terminal tail unfolds and promotes pore forming. The role of IDP in membrane protection and remodelling is another contribution to the ‘ultrastructure’-function relationships.

The polar lipids present in the thylakoid membranes and the inner-chloroplast membrane of eukaryotic microalgae as well as those of cyanobacteria are mainly monogalactosyldiacylglycerols (MGDG), digalactosyldiacylglycerols (DGDG) and sulfoquinovosyldiacylglycerols (SQDG) and a small proportion of phosphatidylglycerol (PG). These represent 70–80% of the total lipids of eukaryotic microalgae that also possess other phospholipids in the extrachloroplastic membranes [115]. In the most studied microalga *C. reinhardtii*, betaine lipids such as diacylglyceryltrimethylhomo-Ser (DGTS) can act as substitute of phosphatidylcholine (PC). The acyl chains of galactolipids from eukaryotic microalgae and cyanobacteria usually differ from those of higher plants by their enrichment in polyunsaturated fatty acids (PUFA) such as  $\alpha$ -linolenic acid (ALA, 18 : 3), the main fatty acid in *C. reinhardtii*, arachidonic acid (ARA; 20 : 4 n-6) and eicosapentaenoic acid (EPA; 20 : 5 n-3) found in *Nannochloropsis gaditana* [116] and *P. tricornutum* [117], docosahexaenoic acid (DHA; 22 : 6 n-3) found in *Schizochytrium limacinum* [118] or hexadecatetraenoic acid (16 : 4 n-3) found in *C. reinhardtii* [115]. Interestingly, lipid biosynthesis in eukaryotic photosynthetic microalgae results from molecular exchanges occurring between different cellular compartments [115,119]. A major part of fatty acid biosynthesis occurs in the stroma of the chloroplast through the action of the fatty acid synthase (FAS) complex on acetyl-CoA as the starting unit further converted in elongated acyl chains by sequential condensation of two-carbon units. Then, acyl chains bound to acyl carrier protein can either be incorporated into acylglycerolipids inside the chloroplast via the so-called ‘prokaryotic’ pathway or be exported outside the chloroplast to reach

the ‘eukaryotic’ pathway in the endoplasmic reticulum (ER). Finally, their incorporation in acyl lipids is performed by various acyl transferases. Approximately 40% of fatty acids synthesised in chloroplasts enter the prokaryotic pathway, whereas 60% are exported to the eukaryotic pathway. About half of the exported fatty acids returns to the plastid after their desaturation in the ER and is used for the synthesis of the thylakoid membrane galactolipids by MGDG and DGDG synthases [120]. Desaturation of fatty acids is tightly linked with the location of the diacylglycerolipids in which they are incorporated and their transfer between the chloroplast envelope and the ER. These fatty acids result from a combination of elongation and desaturation reactions taking place either in the ER where the  $\Delta 6$ - or  $\Delta 5$ -the desaturase are located [121,122], or in the chloroplast where the  $\Delta 4$  desaturase Cr $\Delta 4$ FAD [123] acts on MGDG to generate the 16 : 4  $\Delta 4,7,10,13$  PUFA, a predominant component of MGDG molecular species.

The polar head and fatty acid compositions of the acylglycerol lipids determine their supramolecular organisation [110–112]. While DGDGs are known to form lamellar phases ( $L_{\alpha}$ ) and induce bilayer formation, MGDGs tend to form inverted hexagonal phase ( $H_{II}$ ) in aqueous solution [112]. Because of MGDG physicochemical properties, the formation of photosynthetic membrane bilayer *in vivo* raises questions about the role of this lipid in the organisation and functional properties of the chloroplast membranes [124]. It has been suggested that MGDG, which has a conical molecular shape due to its small head group, may help pack large protein complexes into biological membranes through lipid–protein interactions [113]. The molar ratio of MGDG over DGDG is known to adapt to stress conditions and to modulate the photosynthesis efficiency [125]. Conversely, fatty acid desaturation depends on the photosynthetic activity and the molecular composition of galactolipids varies according to the growth conditions. The high content of PUFAs in galactolipids contributes to the fluidity of membranes [109]. Lipidomics has provided a rich database of the lipid composition of photosynthetic membranes [126]. Critical physical and thermodynamic properties such as bilayer thickness, 2D motions of lipids, packing of the acyl chains, surface charge distribution and thylakoid membrane packing have been characterised using reconstituted galactolipid membranes and a range of methods such as microscopy, differential scanning calorimetry, solid-state NMR, fluorescence anisotropy, small-angle neutron and X-ray scattering, atomic force spectroscopy and molecular dynamics (reviewed here [109]).

The phase separations possibly occurring in these membranes have also been investigated by tensiometry,



ellipsometry and Langmuir–Blodgett transfer coupled to atomic force microscopy using biomimetic Langmuir monolayers [127]. Enzymes (lipases) interacting with monolayers were found to be preferentially adsorbed at the expanded/fluid lipid phases but compounds such as phytosterols and phospholipids inducing phase heterogeneity also favoured the adsorption of enzymes at the phase boundaries and towards the defects in condensed phases. Thus, the lipid composition of photosynthetic membranes affects both the structure of integral membrane proteins from photosystems and the binding of peripheral proteins.

### Other chloroplast microcompartments

Another feature of the chloroplast lipids is that they constitute the boundaries of plastoglobules [54]. The function of these organic phase droplets encompassed by the external thylakoid membrane protuberance is still a matter of debate. It has been proposed that they serve as a reservoir for the maintenance of the protein/galactolipid ratio of the thylakoids, or that their organic phase enables the storage of organic metabolites produced in the chloroplast [36]. In *C. reinhardtii*, recent cryomicroscopy tomograms suggest that their proximity with the thylakoid stack is not obvious [17]. They share some similarities with the eyespots, which are also LDs that locate at the periphery of the chloroplast towards the light. The molecular composition of the plastoglobules and the eyespot is not clear, except that they are phase separated from the chloroplast stroma. They contain mainly prenylquinones and carotenoids and lower amounts of TAGs [128,129]. A protocol for their isolation has been proposed in 2022 that may lift a hurdle for their molecular characterisation [130].

One interesting perspective would be to consider the fact that many metabolites produced in the chloroplast in large quantities form natural deep eutectic solvents (NaDES). These mixtures characterised by a fusion point lower than those of their isolated components are liquid at physiological temperature and they present peculiar solvation properties [131–133]. This is the case for instance for Glucose : Fructose, Fructose : Sucrose, Glucose : Sucrose, Sucrose : Glucose : Fructose at molar ratio [133]. *In vitro* reconstitution of these mixtures studied by NMR showed that in the fluid phase, intermolecular transient contacts act as in liquid crystal to partially order the molecule orientation whilst offering a high fluidity. Chemists have described the good solvation properties of synthetic DES and NaDES for poorly soluble molecules [134,135].

### Carbon and energy storage: starch granules and lipid droplets

In the chloroplast, the main carbon storage components are large polysaccharide condensates in the form of a highly organised semicrystalline fraction: the starch or chrysolaminarin granules. These are ordered polymers of polysaccharide where glucose subunits are predominantly linked by  $\alpha$ -(1  $\rightarrow$  4)-D glycosidic bonds with  $\alpha$ -(1  $\rightarrow$  6) branches for starch and by  $\beta$ -(1  $\rightarrow$  3) and  $\beta$ -(1  $\rightarrow$  6) branches in chrysolaminarin. The starch granules result from a complex organisation of semicrystalline and amorphous concentric layers surrounding an amorphous hilum, and different models have been proposed for their assemblies [27–29]. Contrary to glycogen that is water-soluble and occurs as nanoparticles of limited diameter, the starch/chrysolaminarin molecules can have in principle unlimited size [136]. In the green lineage, starch biogenesis is located in the chloroplast, whereas in the red lineage such as in diatoms, chrysolaminarin synthesis occurs in the vacuole, another membrane-bound microcompartment of the cytosol [137]. The understanding of gluconeogenesis or glycolysis is mainly achieved via genetic studies [138], and recent biophysical tools are being used to explore the molecular structure of this large ordered semicrystalline condensate [139].

The gluconeogenesis *vs* glycolysis equilibrium is dependent on the availability of the energy source, primarily ATP and NAD(P)H, and the several regulation pathways involve exchange through the several microcompartments within the stroma discussed above, but also exchange in and out of the chloroplast in eukaryotic algae. This will be discussed in the next section.

Another form of carbon storage compartment much studied in microalgae is the LD. This is the most effective form of energy storage with 9 kcal·g<sup>-1</sup> for fatty acid and derived acylglycerolipids against 4 kcal·g<sup>-1</sup> for carbohydrates. The most common type of LD presents a hydrophobic core made of TAG and surrounded by a lipoproteic monolayer. *Chlamydomonas reinhardtii* LDs contain 95% TAGs, 1–5% polar lipids and 1–5% proteins [140]. The polar lipid monolayer surrounding the LDs contains a specific set of polar lipids including DGTS, SQDG, DGDG and MGDG with relative amounts depending on culture conditions (light level, nitrogen depletion) [141]. Also at the monolayer, LD proteomics has revealed the presence of enzymes involved in several subcellular mechanisms, including lipid synthesis, degradation, trafficking, signalling and lipid homeostasis. For example, in *C. reinhardtii*, LD proteomics has shown that around 30 proteins involved in lipid metabolism were present,

including the betaine lipid synthase (BTA1), a lysophosphatidic acid acyltransferase (LPAT), a putative long chain acyl-CoA synthetase (LACS), a diacylglycerol acyltransferase (DGAT), a major LD protein (MLDP) of unknown function, the phosphatidylethanolamine-binding DTH1 (DELAYED IN TAG HYDROLYSIS1), two lipases and two enzymes involved in fatty acid  $\beta$ -oxidation [141–143]. This has led to the classification of LDs as new cellular organelles [30].

Triacylglycerol biogenesis regulation is complex, and often triggered by stress conditions such as heat or nutrients depletion (e.g. nitrogen) [26,126]. In *C. reinhardtii*, TAG biosynthesis is thought to mainly occur in the cytosol through the same enzymatic steps as in plants [144], and it requires the transfer to the cytosol of the acyl chains initially synthesised in the chloroplast. Galactolipids also appear as the main backbone in which *de novo*-synthesised fatty acids are incorporated before they enter into TAG synthesis. In *C. reinhardtii*, a galactolipase, named plastid galactoglycerolipid degradation 1 (PGD1), was identified as a key player in lipid remodelling following nitrogen deprivation. The galactolipase activity of PGD1 allows the flux of fatty acids from plastid lipids to TAGs in which they are re-esterified to form LDs [145]. It remains however unclear whether the final step of TAG synthesis from diacylglycerol (DAG) also occurs inside the chloroplast. Indeed, some TAG-synthesising enzymes such as DGAT1 and phosphoglycerol acyltransferase (PDAT) were found in the chloroplast [146]. Also, data from microscopy studies have showed that some LDs can be present inside the chloroplast, as well as in the cytosol in close association with the chloroplast envelope [146,147]. In the chloroplast, LD are referred to as plastoglobules, and we have seen above in [ATP and reducing power generation](#) section, that these contain TAG. Lipid droplet synthesis can yet be another function of these enigmatic microcompartments. We have also seen previously in [ATP and reducing power generation](#) section, that polar lipids from membranes can serve as a source of recycled acyl chains for TAG synthesis, besides *de novo* fatty acid synthesis.

The study of LD biogenesis and composition is typically investigated using timely resolved culture sampling and lipid extraction combined with genetic modification [126]. Nevertheless, these techniques require cellular disruption before isolation of LDs and lipid extraction. These steps can generate side reactions such as lipid hydrolysis/degradation due to their mixing with lipolytic enzymes initially present in other cell compartments, and binding to LDs of amphiphilic proteins that are normally not interacting with LDs.

There is therefore a need for other methods allowing the identification and structural characterisation of lipids and proteins within the cell. One common approach is the expression of green fluorescent protein (GFP)-fused protein to localise the protein using fluorescence confocal microscopy and confirm whether it is effectively bound to LDs *in cellula*. Regarding lipids, an emerging methodology using NMR allowed to investigate the accumulation of TAG in the microalga *N. gaditana* [148]. This nondestructive approach allows real-time analysis of lipids in the living algae, without the need of lipid extraction and separation. As discussed above for protein-NMR, NMR can provide information on the chemistry of lipids such as TAG, but also on the physicochemical properties of their supramolecular organisation. For example, the dynamics of LD formation (size changes) in *P. tricornutum*, as well as the lipid-motion within the cells, were monitored by pulse field gradient nuclear magnetic resonance [149].

The two main forms of carbon storage are antagonistic and correlated. In *C. reinhardtii*, as in other species, fatty acid degradation takes place in the peroxisome, that are small organelles in the cytosol, via  $\beta$ -oxidation [150]. The generated acetyl-CoA can be further converted to carbohydrates serving as building blocks or cellular energy through respiration in the mitochondria. This pathway requires a close connexion between LDs and peroxisome to enable the transfer of the fatty acid released from LDs' TAG by lipases. Also, this pathway is linked to the global energetic balance within the cell that implies exchange between organelles.

## Exchange of metabolites across the boundaries of organelles

We discussed above the apparent energy unbalance between the production by the LEF (ATP/NADPH ratio of 1.3) and the consumption by CO<sub>2</sub> uptake and the CBB cycle (ATP/NADPH ratio of 2.6). Many other metabolic pathways have been described that modulate the ATP/NADPH ratio, which will not be described here (for review refer to [105]). In eukaryotic algae, the energetic balance occurs between the chloroplast, the mitochondria and the cytosol. Organelle membranes are impermeable to NAD(P)H, and various transporters have been identified together with malate and oxaloacetate transporters [151]. Malate conversion to oxaloacetate by malate dehydrogenase generates reducing power; thus, it is established that the malate/oxaloacetate shuttle through the different cellular compartments is a key factor for their

energetic balance. Malate dehydrogenases are located in the chloroplast, in peroxisome (also named glyoxysomes in *C. reinhardtii* [152]), in the cytoplasm and in the mitochondria. Various other transporters also contribute to the maintenance of the metabolic flux, such as inorganic phosphate, ammonium and nitrate/nitrite transporters [153]. Bicarbonate transporters have been discussed above in **Pyrenoid and carboxysome** section. Also concerning the carbon flux, several sugar transporters are present with specialised functions. For example, the triose phosphate transporter 3 has been described as being essential for the metabolic balance and the export of photosynthetic fixed carbon in green algae [154].

The case of diatoms is more complex because of their evolutionary origin, their chloroplast is surrounded by four membranes. Metabolic exchange between the mitochondria and the chloroplast involves direct exchange between the two organelles through their membranes [19,155]. Membranes of intra- and extracellular vesicles have also been identified as shuttles for transferring information, function and metabolites from cellular compartments and the endosomal trafficking system to other cells and tissues. Still concerning lipids, LDs have been shown to interact with other organelles such as the peroxisomes, the nucleus, the mitochondria and involved in metabolite trafficking [140,150].

Metabolic exchange across organelles is also an example of how the existence of microcompartment modulates the metabolism. To fully understand the energetic balance within the cell, one would like to be able to follow the fate of a metabolite from its synthesis to its conversion. Whilst this challenge remains unrealistic at the single molecule level, progress in fluxomic methods provides precious data to improve the current models [156,157]. Fluxomic or 'flux-metabolomics' enable to characterise the metabolic pathway downstream of an isotopically labelled metabolite using mass spectrometry or NMR. Mass spectrometry enables the characterisation of a high number of metabolites on a wide concentration range and thus provides a huge metabolic flux database [158]. Nuclear magnetic resonance has suffered for some time from a lower sensitivity, but it provides the advantage of being nondestructive, as opposed to mass spectrometry, and is not dependent on extraction using different solvents [159,160]. As discussed above for the on-flow monitoring of TAG accumulation, *in-situ* NMR can also be used to monitor the fate of specific metabolites [161–163].

The boundaries of the different microcompartments are where metabolite exchange occurs at their

interfaces. These boundaries are usually biological membranes where receptors and transporters are present in the form of integral membrane proteins, as well as peripheral proteins that bind to the membrane upon fulfilling their task as molecular shuttle or enzymes. In LDs, the monolayer surrounding the hydrophobic core also contains functional enzymes and structural proteins, such as MLDP in *C. reinhardtii*, that control the biogenesis and fate of these organelles. Such interfaces have been extensively studied in the case of LDs/emulsions dispersed in an aqueous phase [164–167]. The concepts of phase separation, interfacial tension, adsorption and partitioning occurring at the lipid-water interface are well-defined. Interfacial tension, or surface pressure, for instance, has an impact on protein and metabolite adsorption and penetration at the interface, enzyme activity, as well as on protein folding and stability [168,169]. The surface of polysaccharide granules also contains starch granule-associated proteins that are often starch synthetic enzymes but can have other functions such as modulating the overall properties of the semicrystalline phase [170,171]. The membrane-less organelles formed by LLPS create a novel type of interface between distinct phases. Intracellular phase separation differs however from demixing of oil and water, because the compounds involved in LLPS (proteins, nucleic acids, amino acids, sugars and other small metabolites) are water soluble and the condensates they form are hydrated. The interface delimiting two aqueous phases formed by LLPS should also be considered. Some proteins and other compounds are specifically localised at this interface, where they might impact physicochemical properties (surface tension and surface potential). For example, Starch Granules Abnormal 1 and 2 proteins localise in the pyrenoid in small puncta and are responsible for the association of starch granules at the periphery of the LLPS [172]. Deletion of this protein results in the modification of the volume/surface ratio of the LLPS and induces the formation of several pyrenoid condensates. Strikingly, hyperoxia is also a condition where no starch granules surround pyrenoid, but the number of pyrenoid fraction is not modified [48]. There is limited understanding of the quantitative laws governing solute partitioning into LLPS and adsorption at their interface. Experimental evidence of solute/metabolite partitioning between microcompartments and membranes is also missing [18]. In that context, diffusion-ordered NMR spectroscopy and estimation of diffusion coefficient can provide information on molecules simultaneously present in distinct phases within the cell [73,76,149,173].

## Molecular consequences of the composition of the microcompartments

As discussed above, within a photosynthetic cell, many microcompartments derived from phase separation are currently being described at the physicochemical level: the pyrenoid, the thylakoids bilayer membranes that separate two phases: the lumen and the stroma, the LDs, the semicrystalline starch or chrysolaminarin granules, and others that remain more enigmatic such as the plastoglobules or the eyespots. For long, biochemists considered only two phases in cells: the aqueous phase of cytoplasm and organelles and the hydrophobic environment formed by membrane mono or bilayers. The gradual recognition of subcellular environments with distinct or nonaqueous phase has drastically changed the representation of the cell and its functional compartments. Intracellular LD for instance became considered as organelles and not just energy storage aggregates when proteomics revealed the presence of specific proteins and enzymes, and therefore specific functions, on their surface [30]. The more recent identification of intracellular and intraorganellar LLPS mediated by protein–protein or protein–ribonucleic acid transient contacts opened new perspectives. The import of CO<sub>2</sub> is a telling example. CO<sub>2</sub> solubility is poor in water and suffers from hydration equilibrium that is pH dependent. On the contrary, CO<sub>2</sub> solubility increases in organic phases where ionisation and pH are not relevant. The pyrenoid is an aqueous phase, but dense protein packing could modulate CO<sub>2</sub> solvation properties. Indeed, in the *A. thaliana* AP2C3 LLPS, CO<sub>2</sub> molecules contribute to the molecular packing at the origin of the condensation [67]. Metabolite solubility across these different phases is very likely variable [174]. Chemists have been using phase transfer catalysis for decades. Could phase-transfer catalysis also contribute to regulate the carbon metabolism within microalgae? What are the respective solubilities of CO<sub>2</sub>, sugar phosphate, glyceric acid, carbohydrate or fatty acids in the different microcompartments mentioned above?

One can also consider the effect of these different phases on the actors of the carbon cycle: the proteins. Most structures of globular enzymes have been solved when the proteins were in crystal phase, and this most likely represents their in-cell overall structure. Nevertheless, the high molecular crowding with large proteins reduces the available space for macromolecules of the same size, this phenomenon is known as excluded volume [175,176]. Excluded volume results in restricted molecular diffusion (viscosity) and is likely

to significantly alter the mobility of proteins. Excluded volume effects were also predicted to have a larger impact on IDP than on globular proteins [177]. The conformational ensemble that adopts an IDP in a dilute phase samples large conformations among others, as demonstrated by their large hydrodynamic radius compared with globular proteins of the same molecular mass [178]. In a crowded environment, these extended conformations may be unfavoured because of the excluded volume effect [177]. Several studies on the effect of molecular crowding on IDPs, either *in vitro* using macromolecular crowders (polyethylene glycol, ficoll, dextran, globular proteins) or in cellular environments (*in vivo* or in cell extracts) suggest that this phenomenon is very complex and each IDP or IDR will behave specifically, depending also on the crowding conditions: While a majority of IDPs will keep their disordered properties in a crowded environment, some of them will partially fold, completely fold, or even sometimes become more disordered [179]. The cell is a complex medium and natural molecular crowding results also favours interactions between molecules, likely to modify the affinity of IDPs with their partners. We have highlighted above several examples of IDP that are key regulators for the condensation of several phases: EPYC1, CsoS2 and IM30. In these condensed phases, the concentration of the IDPs can be very high and they can be considered as self-crowders. Recent studies on several such IDPs looking for hypothetical conformational changes upon phase separation suggest that they generally retain their disordered nature, but their dynamics and mobility are slowed down [70–75,77,78]. Key components of the cell may influence these crowding effects and the dynamics of these phase transitions, as ATP, which has been shown when it is highly concentrated in the cell to enhance the solubility of proteins, and thus to act as a crowd controller [179]. Because each compartment has variable constituents, the nature of the molecular crowding is not homogeneous within the cell, the excluded volumes also, and the conformational sampling of dynamic protein is probably specific for each localisation. Besides, the molecular diversity is also restricted in biocondensates that encompass only specific proteins and/or metabolites. Intrinsically disordered proteins have the particularity of interacting with many partners, and compartmentalisation will reduce the presence of several partners to specific localisations [175,176].

These considerations have driven scientists to perform *in cellula* structural investigations of IDPs, and again NMR has proven to be a suitable method. A very complete review of in cell structural investigation



by NMR can be found here [20], and this is a fast expanding field. An attempt to investigate the structural properties of a plant protein within a cell was limited by the requirement of selective isotopic labelling of the target protein against a 'NMR-invisible' background [180]. A first approach is to use total cell lysate that encompasses all the molecular components reorganised by sonication or high pressure to expose them to the isotopically labelled protein [93]. This, however, will not allow to investigate the specificities of distinct microcompartments, which, in contrast, could be approached by the use of purified compartments (purified pyrenoid, purified plastoglobules) or *in vitro* reconstituted LLPS.

## Conclusions

In cyanobacteria and in eukaryotic microalgae, carbon acquisition, assimilation and storage involve various metabolic routes that spread across various cellular microcompartments. CO<sub>2</sub> is the substrate of RuBisCO that is located in the carboxysome, a semicrystalline microcompartment in cyanobacteria, or in the chloroplast stroma or in the pyrenoid, a LLPS biocondensate, in eukaryotic microalgae. The existence of distinct microcompartments with distinct pH ranging from 6.9 (lumen) to 7.9 (cytosol, stroma, pyrenoid) separated by boundaries permeable for CO<sub>2</sub> but not HCO<sub>3</sub><sup>-</sup> (thylakoids), and the presence of CA in each aqueous phase enable the concentration of CO<sub>2</sub> at the vicinity of RuBisCO. The condensation of RuBisCO is also triggered under high O<sub>2</sub> conditions. What is the diffusion of second RuBisCO substrate and the RuBisCO product in and out of these biocondensates? What is RuBisCO catalytic constant in these highly crowded liquid phase? Separated liquid–liquid phases are a fascinating example of supramolecular organisations that can modulate the physiology of a cell. Following the well-studied case of RuBisCO and its substrates, the existence of other distinct supramolecular organisations can be considered. How do enzymes of the CBB cycle organise to optimise both metabolic flux and substrate availability? Several megacomplexes have been proposed in the literature, but are lacking high-resolution structural characterisation. The putative low affinity for these complexes could explain why their reconstitution is challenging. One can also hypothesise the existence of linker proteins that remain to be identified, as this is the case for CP12 that is the linker for the GAPDH-CP12-PRK complex.

CP12 is a conditionally disordered protein with multiple functions but no catalytic activity [12]. A high number of proteins that belong to the IDP family such

as CP12 play a role in the microcompartmentalisation of the cells. They can be scaffold for LLPS demixing (e.g. EPYC1 and CsoS2); sensors to induce the formation of these microcompartments (e.g. AP2C2); or they can contribute to the remodelling of thylakoid membranes (e.g. IM30). Their malleability enables them to adapt to many different phases and interphases that have different physicochemical properties. However, the lack of catalytic activities and their atypical physicochemical properties renders them difficult to identify, and it is likely that more IDPs will be identified in future thanks to advanced omics approaches.

The location of photosynthetic enzymes in a specific organelle, the chloroplast, is known since the middle of the nineteenth century [181,182], and the advantage of physical barriers to confine the toxic O<sub>2</sub> photosynthetic product has been well described. Beyond the membrane-delimited organelles such as the chloroplasts, thylakoid lumen, vacuole, peroxisome, mitochondria or plastoglobules, other intracellular biocondensates such as the pyrenoids or LDs are now emerging. They are not delimited by a lipid bilayer but demix spontaneously due to their chemical composition. Lipid droplets demix because of their lipophilic components and hydrophobic interactions. Protein-rich LLPS demix because of electrostatic interactions and hydrogen bonds. Phase separation, in which solutes self-aggregate but remain in a liquid condensed state, is named coacervation [183]. The biologists' interest for this phenomenon has increased after coacervation was found to occur in cells [32,33], but it has been proposed as one supramolecular organisation as early as the beginning of the twentieth century [184]. Indeed, Oparin hypothesised that life could have emerged under the form of spontaneous coacervates before the occurrence of long amphiphilic lipids [184,185]. Strikingly, we now know that fatty acid synthesis and desaturation involve multiple exchanges in and out of microcompartments of the chloroplast and out of the chloroplast: ER, peroxisomes, mitochondria.

Investigating the structure and function of proteins in such environments is challenging, but it will certainly reveal a novel and better understanding of biological reactions and metabolic pathways. Recent advances in microscopy and spectroscopic methods, and the opportunity to perform molecular scale analysis on living cell by *in-vivo* fluorescent and in-cell spectroscopic methods such as NMR and EPR [20,186] have opened new perspectives. Nuclear magnetic resonance spectroscopy and its various applications appear as the most powerful biophysical methods to investigate *in cellula* and in biomimetic media the structure–



function and ultrastructure–function relationships of enzymes and their cofactors coupled to reaction kinetics and metabolite monitoring. These are exciting objectives that drive research projects in this field.

## Acknowledgements

HL thanks the FEBS Excellence award. Financial support from the CNRS, Aix Marseille University, the French Agence Nationale de la Recherche ANR-22-CE44-0031-01 and ANR-21-CE20-0029 is acknowledged. The authors thank the administrative support of the BIP laboratory, the Institut de Microbiology de la Méditerranée (IMM) and the Institute Microbiology Bioénergies et Biotechnologies (IM2B): Isabelle Pinet, Aurelia Bimbi, Julia Fargeot, Agnes Kammoun, Agnès Duclot.

## References

- Recent work in several fields of science has identified a bias in citation practices such that papers from women and other minority scholars are under-cited relative to the number of such papers in the field [187]. Our list of authors is thus, as many, not representative of the diversity of respected scholars in the fields.
- 1 Le Moigne T, Boisset ND, de Carpentier F, Crozet P, Danon A, Henri J, Marchand CH, Lemaire SD and Johnson X (2023) Chapter 8 – Photoproduction of reducing power and the Calvin-Benson cycle. In *The Chlamydomonas Sourcebook* (Grossman AR and Wollman F-A, eds), 3rd edn, pp. 273–315. Academic Press, London.
- 2 Buchanan BB and Balmer Y (2005) REDOX REGULATION: a broadening horizon. *Annu Rev Plant Biol* **56**, 187–220.
- 3 Jensen E, Clément R, Maberly SC and Gontero B (2017) Regulation of the Calvin-Benson-Bassham cycle in the enigmatic diatoms: biochemical and evolutionary variations on an original theme. *Philos Trans R Soc Lond B Biol Sci* **372**, 20160401.
- 4 Launay H, Huang W, Maberly SC and Gontero B (2020) Regulation of carbon metabolism by environmental conditions: a perspective from diatoms and other chromalveolates. *Front Plant Sci* **11**, 1033.
- 5 Zimmer D, Swart C, Graf A, Arrivault S, Tillich M, Proost S, Nikoloski Z, Stitt M, Bock R, Mühlhaus T *et al.* (2021) Topology of the redox network during induction of photosynthesis as revealed by time-resolved proteomics in tobacco. *Sci Adv* **7**, eabi8307.
- 6 Michelet L, Zaffagnini M, Morisse S, Sparla F, Pérez-Pérez ME, Francia F, Danon A, Marchand CH, Fermani S, Trost P *et al.* (2013) Redox regulation of the Calvin-Benson cycle: something old, something new. *Front Plant Sci* **4**, 470.
- 7 Stec B (2012) Structural mechanism of RuBisCO activation by carbamylation of the active site lysine. *Proc Natl Acad Sci USA* **109**, 18785–18790.
- 8 Gütle DD, Roret T, Müller SJ, Couturier J, Lemaire SD, Hecker A, Dhalleine T, Buchanan BB, Reski R, Einsle O *et al.* (2016) Chloroplast FBPase and SBPase are thioredoxin-linked enzymes with similar architecture but different evolutionary histories. *Proc Natl Acad Sci USA* **113**, 6779–6784.
- 9 Gurrieri L, Del Giudice A, Demitri N, Falini G, Pavel NV, Zaffagnini M, Polentarutti M, Crozet P, Marchand CH, Henri J *et al.* (2019) *Arabidopsis* and *Chlamydomonas* phosphoribulokinase crystal structures complete the redox structural proteome of the Calvin-Benson cycle. *Proc Natl Acad Sci USA* **116**, 8048–8053.
- 10 Gontero B, Meunier J-C, Buc J and Ricard J (1984) The ‘slow’ pH-induced conformational transition of chloroplast fructose 1,6-bisphosphatase and the control of the Calvin cycle. *Eur J Biochem* **145**, 485–488.
- 11 Launay H, Receveur-Bréchet V, Carrière F and Gontero B (2019) Orchestration of algal metabolism by protein disorder. *Arch Biochem Biophys* **672**, 108070.
- 12 Gérard C, Carrière F, Receveur-Bréchet V, Launay H and Gontero B (2022) A trajectory of discovery: metabolic regulation by the conditionally disordered chloroplast protein, CP12. *Biomolecules* **12**, 1047.
- 13 Gontero B, Cárdenas ML and Ricard J (1988) A functional five-enzyme complex of chloroplasts involved in the Calvin cycle. *Eur J Biochem* **173**, 437–443.
- 14 Graciet E, Lebreton S and Gontero B (2004) Emergence of new regulatory mechanisms in the Benson-Calvin pathway via protein-protein interactions: a glyceraldehyde-3-phosphate dehydrogenase/CP12/phosphoribulokinase complex. *J Exp Bot* **55**, 1245–1254.
- 15 Agarwal R, Ortleb S, Sainis JK and Melzer M (2009) Immunoelectron microscopy for locating Calvin cycle enzymes in the thylakoids of *Synechocystis* 6803. *Mol Plant* **2**, 32–42.
- 16 Wang L, Patena W, Baalen KAV, Xie Y, Singer ER, Gavrilenko S, Warren-Williams M, Han L, Harrigan HR, Hartz LD *et al.* (2023) A chloroplast protein atlas reveals punctate structures and spatial organization of biosynthetic pathways. *Cell* **186**, 3499–3518.e14.
- 17 Engel BD, Schaffer M, Kuhn Cuellar L, Villa E, Plitzko JM and Baumeister W (2015) Native architecture of the *Chlamydomonas* chloroplast revealed by in situ cryo-electron tomography. *Elife* **4**, e04889.
- 18 Küken A, Sommer F, Yaneva-Roder L, Mackinder LC, Höhne M, Geimer S, Jonikas MC, Schroda M,

- Stitt M, Nikoloski Z *et al.* (2018) Effects of microcompartmentation on flux distribution and metabolic pools in *Chlamydomonas reinhardtii* chloroplasts. *Elife* **7**, e37960.
- 19 Uwizeye C, Decelle J, Jouneau P-H, Flori S, Gallet B, Keck J-B, Bo DD, Moriscot C, Seydoux C, Chevalier F *et al.* (2021) Morphological bases of phytoplankton energy management and physiological responses unveiled by 3D subcellular imaging. *Nat Commun* **12**, 1049.
  - 20 Theillet F-X and Luchinat E (2022) In-cell NMR: why and how? *Prog Nucl Magn Reson Spectrosc* **132–133**, 1–112.
  - 21 Taylor MJ, Lukowski JK and Anderton CR (2021) Spatially resolved mass spectrometry at the single cell: recent innovations in proteomics and metabolomics. *J Am Soc Mass Spectrom* **32**, 872–894.
  - 22 Gruber A, Weber T, Bártulos CR, Vugrinec S and Kroth PG (2009) Intracellular distribution of the reductive and oxidative pentose phosphate pathways in two diatoms. *J Basic Microbiol* **49**, 58–72.
  - 23 Cenci U, Chabi M, Ducatez M, Tirtiaux C, Nirmal-Raj J, Utsumi Y, Kobayashi D, Sasaki S, Suzuki E, Nakamura Y *et al.* (2013) Convergent evolution of polysaccharide debranching defines a common mechanism for starch accumulation in cyanobacteria and plants. *Plant Cell* **25**, 3961–3975.
  - 24 Wilhelm C, Büchel C, Fisahn J, Goss R, Jakob T, LaRoche J, Lavaud J, Lohr M, Riebesell U, Stehfest K *et al.* (2006) The regulation of carbon and nutrient assimilation in diatoms is significantly different from green algae. *Protist* **157**, 91–124.
  - 25 Allan GG, Lewin J and Johnson PG (1972) Marine polymers. IV diatom polysaccharides. *Botanica Marina* **15**, 102–108.
  - 26 Li-Beisson Y and Carrière F (2020) Biogenesis and fate of lipid droplets. *Biochimie* **169**, 1–2.
  - 27 Buléon A, Colonna P, Planchot V and Ball S (1998) Starch granules: structure and biosynthesis. *Int J Biol Macromol* **23**, 85–112.
  - 28 Pérez S and Bertoft E (2010) The molecular structures of starch components and their contribution to the architecture of starch granules: a comprehensive review. *Starke* **62**, 389–420.
  - 29 Tetlow IJ and Bertoft E (2020) A review of starch biosynthesis in relation to the building block-backbone model. *Int J Mol Sci* **21**, 7011.
  - 30 Cohen S (2018) Lipid droplets as organelles. *Int Rev Cell Mol Biol* **337**, 83–110.
  - 31 Banani SF, Lee HO, Hyman AA and Rosen MK (2017) Biomolecular condensates: organizers of cellular biochemistry. *Nat Rev Mol Cell Biol* **18**, 285–298.
  - 32 Spruijt E (2023) Open questions on liquid–liquid phase separation. *Commun Chem* **6**, 1–5.
  - 33 Boeynaems S, Alberti S, Fawzi NL, Mittag T, Polymenidou M, Rousseau F, Schymkowitz J, Shorter J, Wolozin B, Van Den Bosch L *et al.* (2018) Protein phase separation: a new phase in cell biology. *Trends Cell Biol* **28**, 420–435.
  - 34 Cable J, Brangwynne C, Seydoux G, Cowburn D, Pappu RV, Castañeda CA, Berchowitz LE, Chen Z, Jonikas M, Dernburg A *et al.* (2019) Phase separation in biology and disease—a symposium report. *Ann N Y Acad Sci* **1452**, 3–11.
  - 35 Rae BD, Long BM, Badger MR and Price GD (2013) Functions, compositions, and evolution of the two types of carboxysomes: polyhedral microcompartments that facilitate CO<sub>2</sub> fixation in cyanobacteria and some proteobacteria. *Microbiol Mol Biol Rev* **77**, 357–379.
  - 36 van Wijk KJ and Kessler F (2017) Plastoglobuli: plastid microcompartments with integrated functions in metabolism, plastid developmental transitions, and environmental adaptation. *Annu Rev Plant Biol* **68**, 253–289.
  - 37 Arzac MI, Fernández-Marín B and García-Plazaola JJ (2022) More than just lipid balls: quantitative analysis of plastoglobule attributes and their stress-related responses. *Planta* **255**, 62.
  - 38 Austin JR, Frost E, Vidi P-A, Kessler F and Staehelin LA (2006) Plastoglobules are lipoprotein subcompartments of the chloroplast that are permanently coupled to thylakoid membranes and contain biosynthetic enzymes. *Plant Cell* **18**, 1693–1703.
  - 39 Tabita FR, Satagopan S, Hanson TE, Kreel NE and Scott SS (2008) Distinct form I, II, III, and IV Rubisco proteins from the three kingdoms of life provide clues about Rubisco evolution and structure/function relationships. *J Exp Bot* **59**, 1515–1524.
  - 40 Andersson I, Knight S, Schneider G, Lindqvist Y, Lundqvist T, Brändén C-I and Lorimer GH (1989) Crystal structure of the active site of ribulose-bisphosphate carboxylase. *Nature* **337**, 229–234.
  - 41 Gontero B and Maberly SC (2022) Biochemical carbon dioxide concentrating mechanisms. In *Blue Planet, Red and Green Photosynthesis* (Maberly S and Gontero B, eds), pp. 133–166. ISTE, London.
  - 42 Stotz M, Mueller-Cajar O, Ciniawsky S, Wendler P, Hartl FU, Bracher A and Hayer-Hartl M (2011) Structure of green-type RuBisCO activase from tobacco. *Nat Struct Mol Biol* **18**, 1366–1370.
  - 43 Mueller-Cajar O, Stotz M, Wendler P, Hartl FU, Bracher A and Hayer-Hartl M (2011) Structure and function of the AAA+ protein CbbX, a red-type RuBisCO activase. *Nature* **479**, 194–199.
  - 44 Meyer MT, Whittaker C and Griffiths H (2017) The algal pyrenoid: key unanswered questions. *J Exp Bot* **68**, 3739–3749.
  - 45 Meyer M and Griffiths H (2013) Origins and diversity of eukaryotic CO<sub>2</sub>-concentrating mechanisms: lessons for the future. *J Exp Bot* **64**, 769–786.

- 46 Meyer MT (2022) Rubisco microcompartments: the function of carboxysomes and pyrenoids in aquatic CO<sub>2</sub>. In *Blue Planet, Red and Green Photosynthesis* (Maberly S and Gontero B, eds), ISTE, London.
- 47 Ramazanov Z, Rawat M, Henk MC, Mason CB, Matthews SW and Moroney JV (1994) The induction of the CO<sub>2</sub>-concentrating mechanism is correlated with the formation of the starch sheath around the pyrenoid of *Chlamydomonas reinhardtii*. *Planta* **195**, 210–216.
- 48 Neofotis P, Temple J, Tessmer OL, Bibik J, Norris N, Pollner E, Lucker B, Weraduwege SM, Withrow A, Sears B *et al.* (2021) The induction of pyrenoid synthesis by hyperoxia and its implications for the natural diversity of photosynthetic responses in *Chlamydomonas*. *Elife* **10**, e67565.
- 49 He S, Chou H-T, Matthies D, Wunder T, Meyer MT, Atkinson N, Martinez-Sanchez A, Jeffrey PD, Port SA, Patena W *et al.* (2020) The structural basis of RuBisCO phase separation in the pyrenoid. *Nat Plants* **6**, 1480–1490.
- 50 Meyer MT, Itakura AK, Patena W, Wang L, He S, Emrich-Mills T, Lau CS, Yates G, Mackinder LCM and Jonikas MC (2020) Assembly of the algal CO<sub>2</sub>-fixing organelle, the pyrenoid, is guided by a Rubisco-binding motif. *Science. Advances* **6**, eabd2408.
- 51 Wunder T, Cheng SLH, Lai S-K, Li H-Y and Mueller-Cajar O (2018) The phase separation underlying the pyrenoid-based microalgal RuBisCO supercharger. *Nat Commun* **9**, 5076.
- 52 Freeman Rosenzweig ES, Xu B, Kuhn Cuellar L, Martinez-Sanchez A, Schaffer M, Strauss M, Cartwright HN, Ronceray P, Plitzko JM, Förster F *et al.* (2017) The eukaryotic CO<sub>2</sub>-concentrating organelle is liquid-like and exhibits dynamic reorganization. *Cell* **171**, 148–162.e19.
- 53 Kirchhoff H (2019) Chloroplast ultrastructure in plants. *New Phytol* **223**, 565–574.
- 54 Shanmugabalaji V, Zita W, Collombat J and Kessler F (2022) Chapter three – plastoglobules: a hub of lipid metabolism in the chloroplast. In *Advances in Botanical Research* (Rébeillé F and Maréchal E, eds), pp. 91–119. Academic Press, Cambridge, MA.
- 55 Boeynaems S, Chong S, Gsponer J, Holt L, Milovanovic D, Mitrea DM, Mueller-Cajar O, Portz B, Reilly JF, Reinkemeier CD *et al.* (2023) Phase separation in biology and disease; current perspectives and open questions. *J Mol Biol* **435**, 167971.
- 56 Bar-On YM and Milo R (2019) The global mass and average rate of RuBisCO. *Proc Natl Acad Sci USA* **116**, 4738–4743.
- 57 Fei C, Wilson AT, Mangan NM, Wingreen NS and Jonikas MC (2022) Modelling the pyrenoid-based CO<sub>2</sub>-concentrating mechanism provides insights into its operating principles and a roadmap for its engineering into crops. *Nat Plants* **8**, 583–595.
- 58 Giordano M, Beardall J and Raven JA (2005) CO<sub>2</sub> concentrating mechanisms in algae: mechanisms, environmental modulation, and evolution. *Annu Rev Plant Biol* **56**, 99–131.
- 59 Huang W, Han S, Jiang H, Gu S, Li W, Gontero B and Maberly SC (2020) External  $\alpha$ -carbonic anhydrase and solute carrier 4 are required for bicarbonate uptake in a freshwater angiosperm. *J Exp Bot* **71**, 6004–6014.
- 60 Long BM, Badger MR, Whitney SM and Price GD (2007) Analysis of carboxysomes from *Synechococcus* PCC7942 reveals multiple Rubisco complexes with carboxysomal proteins CcmM and CcaA. *J Biol Chem* **282**, 29323–29335.
- 61 Wang H, Yan X, Aigner H, Bracher A, Nguyen ND, Hee WY, Long BM, Price GD, Hartl FU and Hayer-Hartl M (2019) RuBisCO condensate formation by CcmM in  $\beta$ -carboxysome biogenesis. *Nature* **566**, 131–135.
- 62 Zang K, Wang H, Hartl FU and Hayer-Hartl M (2021) Scaffolding protein CcmM directs multiprotein phase separation in  $\beta$ -carboxysome biogenesis. *Nat Struct Mol Biol* **28**, 909–922.
- 63 Oltrogge LM, Chaijarasphong T, Chen AW, Bolin ER, Marqusee S and Savage DF (2020) Multivalent interactions between CsoS2 and RuBisCO mediate  $\alpha$ -carboxysome formation. *Nat Struct Mol Biol* **27**, 281–287.
- 64 Cameron JC, Wilson SC, Bernstein SL and Kerfeld CA (2013) Biogenesis of a bacterial organelle: the carboxysome assembly pathway. *Cell* **155**, 1131–1140.
- 65 Mackinder LCM, Chen C, Leib RD, Patena W, Blum SR, Rodman M, Ramundo S, Adams CM and Jonikas MC (2017) A spatial interactome reveals the protein organization of the algal CO<sub>2</sub>-concentrating mechanism. *Cell* **171**, 133–147.e14.
- 66 Mackinder LCM, Meyer MT, Mettler-Altmann T, Chen VK, Mitchell MC, Caspari O, Freeman Rosenzweig ES, Pallesen L, Reeves G, Itakura A *et al.* (2016) A repeat protein links RuBisCO to form the eukaryotic carbon-concentrating organelle. *Proc Natl Acad Sci USA* **113**, 5958–5963.
- 67 Zhang M, Zhu C, Duan Y, Liu T, Liu H, Su C and Lu Y (2022) The intrinsically disordered region from PP2C phosphatases functions as a conserved CO<sub>2</sub> sensor. *Nat Cell Biol* **24**, 1029–1037.
- 68 Harrison RES, Weng K, Wang Y and Peng Q (2021) Phase separation and histone epigenetics in genome regulation. *Curr Opin Solid State Mater Sci* **25**, 100892.
- 69 Kuznetsova IM, Zaslavsky BY, Breydo L, Turoverov KK and Uversky VN (2015) Beyond the excluded volume effects: mechanistic complexity of the crowded milieu. *Molecules* **20**, 1377–1409.

- 70 Murthy AC, Dignon GL, Kan Y, Zerze GH, Parekh SH, Mittal J and Fawzi NL (2019) Molecular interactions underlying liquid–liquid phase separation of the FUS low-complexity domain. *Nat Struct Mol Biol* **26**, 637–648.
- 71 Ryan VH, Dignon GL, Zerze GH, Chabata CV, Silva R, Conicella AE, Amaya J, Burke KA, Mittal J and Fawzi NL (2018) Mechanistic view of hnRNPA2 low complexity domain structure, interactions, and phase separation altered by disease mutation and arginine methylation. *Mol Cell* **69**, 465–479.e7.
- 72 Wong LE, Kim TH, Muhandiram DR, Forman-Kay JD and Kay LE (2020) NMR experiments for studies of dilute and condensed protein phases: application to the phase-separating protein CAPRIN1. *J Am Chem Soc* **142**, 2471–2489.
- 73 Brady JP, Farber PJ, Sekhar A, Lin Y-H, Huang R, Bah A, Nott TJ, Chan HS, Baldwin AJ, Forman-Kay JD *et al.* (2017) Structural and hydrodynamic properties of an intrinsically disordered region of a germ cell-specific protein on phase separation. *Proc Natl Acad Sci USA* **114**, E8194–E8203.
- 74 Ackermann BE and Debelouchina GT (2019) Heterochromatin protein HP1 $\alpha$  gelation dynamics revealed by solid-state NMR spectroscopy. *Angew Chem Int Ed Engl* **58**, 6300–6305.
- 75 Ambadipudi S, Biernat J, Riedel D, Mandelkow E and Zweckstetter M (2017) Liquid–liquid phase separation of the microtubule-binding repeats of the Alzheimer-related protein tau. *Nat Commun* **8**, 275.
- 76 Pantoja CF, Ibáñez de Opakua A, Cima-Omori M-S and Zweckstetter M (2023) Determining the physicochemical composition of biomolecular condensates from spatially-resolved NMR. *Angew Chem Int Ed Engl* **62**, e202218078.
- 77 Guseva S, Schnapka V, Adamski W, Maurin D, Ruigrok RWH, Salvi N and Blackledge M (2023) Liquid-liquid phase separation modifies the dynamic properties of intrinsically disordered proteins. *J Am Chem Soc* **145**, 10548–10563.
- 78 Mohanty P, Shenoy J, Rizuan A, Ortiz JFM, Fawzi NL and Mittal J (2022) Aliphatic residues contribute significantly to the phase separation of TDP-43 C-terminal domain. *bioRxiv* [10.1101/2022.11.10.516004](https://doi.org/10.1101/2022.11.10.516004) [PREPRINT]
- 79 Ikeya T, Ban D, Lee D, Ito Y, Kato K and Griesinger C (2018) Solution NMR views of dynamical ordering of biomacromolecules. *Biochim Biophys Acta Gen Subj* **1862**, 287–306.
- 80 Yamori W, Evans JR and Von Caemmerer S (2010) Effects of growth and measurement light intensities on temperature dependence of CO<sub>2</sub> assimilation rate in tobacco leaves. *Plant Cell Environ* **33**, 332–343.
- 81 Paul MJ, Knight JS, Habash D, Parry MAJ, Lawlor DW, Barnes SA, Loynes A and Gray JC (1995) Reduction in phosphoribulokinase activity by antisense RNA in transgenic tobacco: effect on CO<sub>2</sub> assimilation and growth in low irradiance. *Plant J* **7**, 535–542.
- 82 Boisset ND, Favoino G, Meloni M, Jomat L, Cassier-Chauvat C, Zaffagnini M, Lemaire SD and Crozet P (2023) Phosphoribulokinase abundance is not limiting the Calvin-Benson-Bassham cycle in *Chlamydomonas reinhardtii*. *bioRxiv* [10.1101/2023.05.10.540127](https://doi.org/10.1101/2023.05.10.540127) [PREPRINT]
- 83 Fridlyand LE and Scheibe R (1999) Regulation of the Calvin cycle for CO<sub>2</sub> fixation as an example for general control mechanisms in metabolic cycles. *Biosystems* **51**, 79–93.
- 84 McFarlane C, Shah N, Kabasakal BV, Cotton CAR, Bubeck D and Murray JW (2019) Structural basis of light-induced redox regulation in the Calvin cycle. *Proc Natl Acad Sci USA* **116**, 20984–20990.
- 85 Yu A, Xie Y, Pan X, Zhang H, Cao P, Su X, Chang W and Li M (2020) Photosynthetic phosphoribulokinase structures: enzymatic mechanisms and the redox regulation of the Calvin-Benson-Bassham cycle. *Plant Cell* **32**, 1556–1573.
- 86 Wilson RH, Hayer-Hartl M and Bracher A (2019) Crystal structure of phosphoribulokinase from *Synechococcus* sp. strain PCC 6301. *Acta Crystallogr F Struct Biol Commun* **75**, 278–289.
- 87 Marri L, Zaffagnini M, Collin V, Issakidis-Bourguet E, Lemaire SD, Pupillo P, Sparla F, Miginiac-Maslow M and Trost P (2009) Prompt and easy activation by specific thioredoxins of Calvin cycle enzymes of *Arabidopsis thaliana* associated in the GAPDH/CP12/PRK supramolecular complex. *Mol Plant* **2**, 259–269.
- 88 Avilan L, Lebreton S and Gontero B (2000) Thioredoxin activation of phosphoribulokinase in a bi-enzyme complex from *Chlamydomonas reinhardtii* chloroplasts. *J Biol Chem* **275**, 9447–9451.
- 89 Porter MA, Stringer CD and Hartman FC (1988) Characterization of the regulatory thioredoxin site of phosphoribulokinase. *J Biol Chem* **263**, 123–129.
- 90 Roesler KR, Marcotte BL and Ogren WL (1992) Functional importance of arginine 64 in *Chlamydomonas reinhardtii* phosphoribulokinase. *Plant Physiol* **98**, 1285–1289.
- 91 Graciet E, Gans P, Wedel N, Lebreton S, Camadro J-M and Gontero B (2003) The small protein CP12: a protein linker for supramolecular complex assembly. *Biochemistry* **42**, 8163–8170.
- 92 Lebreton S, Graciet E and Gontero B (2003) Modulation, via protein-protein interactions, of glyceraldehyde-3-phosphate dehydrogenase activity through redox phosphoribulokinase regulation. *J Biol Chem* **278**, 12078–12084.
- 93 Launay H, Shao H, Bornet O, Cantrelle F-X, Lebrun R, Receveur-Brechot V and Gontero B (2021) Flexibility of oxidized and reduced states of the

- chloroplast regulatory protein CP12 in isolation and in cell extracts. *Biomolecules* **11**, 701.
- 94 Lebreton S and Gontero B (1999) Memory and imprinting in multienzyme complexes. Evidence for information transfer from glyceraldehyde-3-phosphate dehydrogenase to phosphoribulokinase under reduced state in *Chlamydomonas reinhardtii*. *J Biol Chem* **274**, 20879–20884.
  - 95 Marri L, Thieulin-Pardo G, Lebrun R, Puppo R, Zaffagnini M, Trost P, Gontero B and Sparla F (2014) CP12-mediated protection of Calvin–Benson cycle enzymes from oxidative stress. *Biochimie* **97**, 228–237.
  - 96 Erales J, Avilan L, Lebreton S and Gontero B (2008) Exploring CP12 binding proteins revealed aldolase as a new partner for the phosphoribulokinase/glyceraldehyde 3-phosphate dehydrogenase/CP12 complex – purification and kinetic characterization of this enzyme from *Chlamydomonas reinhardtii*. *FEBS J* **275**, 1248–1259.
  - 97 Süss K-H, Arkona C, Manteuffel R and Adler K (1993) Calvin cycle multienzyme complexes are bound to chloroplast thylakoid membranes of higher plants in situ. *Proc Natl Acad Sci USA* **90**, 5514–5518.
  - 98 Mendiola L and Akazawa T (1964) Partial purification and the enzymatic nature of fraction I protein of rice leaves. *Biochemistry* **3**, 174–179.
  - 99 Van Noort G and Wildman SG (1964) Proteins of green leaves: IX. Enzymatic properties of fraction-I protein isolated by a specific antibody. *Biochim Biophys Acta Gen Subj* **90**, 309–317.
  - 100 Gontero B, Giudici-Ortoni M-T and Ricard J (1994) The modulation of enzyme reaction rates within multi-enzyme complexes. *Eur J Biochem* **226**, 999–1006.
  - 101 Pohlmeier K, Paap BK, Soll J and Wedel N (1996) CP12: a small nuclear-encoded chloroplast protein provides novel insights into higher-plant GAPDH evolution. *Plant Mol Biol* **32**, 969–978.
  - 102 Piersimoni L, Kastritis PL, Arlt C and Sinz A (2022) Cross-linking mass spectrometry for investigating protein conformations and protein–protein interactions—a method for all seasons. *Chem Rev* **122**, 7500–7531.
  - 103 Walker BJ, Kramer DM, Fisher N and Fu X (2020) Flexibility in the energy balancing network of photosynthesis enables safe operation under changing environmental conditions. *Plan Theory* **9**, 301.
  - 104 Shikanai T and Yamamoto H (2017) Contribution of cyclic and pseudo-cyclic electron transport to the formation of proton motive force in chloroplasts. *Mol Plant* **10**, 20–29.
  - 105 Dao O, Kuhnert F, Weber APM, Peltier G and Li-Beisson Y (2022) Physiological functions of malate shuttles in plants and algae. *Trends Plant Sci* **27**, 488–501.
  - 106 Dekker JP and Boekema EJ (2005) Supramolecular organization of thylakoid membrane proteins in green plants. *Biochim Biophys Acta Bioenerg* **1706**, 12–39.
  - 107 Olive J, Vallon O, Wollman F-A, Recouvreur M and Bennoun P (1986) Studies on the cytochrome b 6/f complex. II. Localization of the complex in the thylakoid membranes from spinach and *Chlamydomonas reinhardtii* by immunocytochemistry and freeze-fracture analysis of b 6/f mutants. *Biochim Biophys Acta Bioenerg* **851**, 239–248.
  - 108 Rathod AK, Chavda D and Manna M (2023) Phase transition and phase separation in realistic thylakoid lipid membrane of marine algae in all-atom simulations. *J Chem Inf Model* **63**, 3328–3339.
  - 109 Bolik S, Demé B and Jouhet J (2022) Chapter one – biophysical properties of glycerolipids and their impact on membrane architecture and biology. In *Advances in Botanical Research* (Rébeillé F and Maréchal E, eds), pp. 1–57. Academic Press, Cambridge, MA.
  - 110 Siebenaller C and Schneider D (2023) Cyanobacterial membrane dynamics in the light of eukaryotic principles. *Biosci Rep* **43**, BSR20221269.
  - 111 Bottier C, Géan J, Artzner F, Desbat B, Pézolet M, Renault A, Marion D and Vié V (2007) Galactosyl headgroup interactions control the molecular packing of wheat lipids in Langmuir films and in hydrated liquid-crystalline mesophases. *Biochim Biophys Acta* **1768**, 1526–1540.
  - 112 Brentel I, Selstam E and Lindblom G (1985) Phase equilibria of mixtures of plant galactolipids. The formation of a bicontinuous cubic phase. *Biochim Biophys Acta Biomembr* **812**, 816–826.
  - 113 Israelachvili JN, Marcelja S and Horn RG (1980) Physical principles of membrane organization. *Q Rev Biophys* **13**, 121–200.
  - 114 Junglas B, Orru R, Axt A, Siebenaller C, Steinchen W, Heidrich J, Hellmich UA, Hellmann N, Wolf E, Weber SAL *et al.* (2020) IM30 IDPs form a membrane-protective carpet upon super-complex disassembly. *Commun Biol* **3**, 595.
  - 115 Li-Beisson Y, Beisson F and Riekhof W (2015) Metabolism of acyl-lipids in *Chlamydomonas reinhardtii*. *Plant J* **82**, 504–522.
  - 116 Sukenik A, Zmora O and Carmeli Y (1993) Biochemical quality of marine unicellular algae with special emphasis on lipid composition. II *Nannochloropsis* Sp. *Aquaculture* **117**, 313–326.
  - 117 Jensen EL, Yangüez K, Carrière F and Gontero B (2020) Storage compound accumulation in diatoms as response to elevated CO<sub>2</sub> concentration. *Biology* **9**, 5.
  - 118 Talbierz S, Dębowski M, Kujawska N, Kazimierowicz J and Zieliński M (2022) Optimization of lipid production by *Schizochytrium limacinum* biomass modified with ethyl methane sulfonate and grown on



- waste glycerol. *Int J Environ res Public Health* **19**, 3108.
- 119 Li-Beisson Y, Shorrosh B, Beisson F, Andersson MX, Arondel V, Bates PD, Baud S, Bird D, DeBono A, Durrett TP *et al.* (2010) Acyl-lipid metabolism. *Arabidopsis Book* **8**, e0133.
  - 120 Browse J, Warwick N, Somerville CR and Slack CR (1986) Fluxes through the prokaryotic and eukaryotic pathways of lipid synthesis in the “16:3” plant *Arabidopsis thaliana*. *Biochem J* **235**, 25–31.
  - 121 Shi H, Wu R, Zheng Y and Yue X (2018) Molecular mechanisms underlying catalytic activity of delta 6 desaturase from *Glossomastix chrysoplata* and *Thalassiosira pseudonana*. *J Lipid res* **59**, 79–88.
  - 122 Kajikawa M, Yamato KT, Kohzu Y, Shoji S, Matsui K, Tanaka Y, Sakai Y and Fukuzawa H (2006) A front-end desaturase from *Chlamydomonas reinhardtii* produces pinolenic and coniferonic acids by omega13 desaturation in methylotrophic yeast and tobacco. *Plant Cell Physiol* **47**, 64–73.
  - 123 Zäuner S, Jochum W, Bigorowski T and Benning C (2012) A cytochrome b5-containing plastid-located fatty acid desaturase from *Chlamydomonas reinhardtii*. *Eukaryot Cell* **11**, 856–863.
  - 124 Gounaris K and Barber J (1983) Monogalactosyldiacylglycerol: the most abundant polar lipid in nature. *Trends Biochem Sci* **8**, 378–381.
  - 125 Li H-M and Yu C-W (2018) Chloroplast galactolipids: the link between photosynthesis, chloroplast shape, jasmonates, phosphate starvation and freezing tolerance. *Plant Cell Physiol* **59**, 1128–1134.
  - 126 Légeret B, Schulz-Raffelt M, Nguyen HM, Auroy P, Beisson F, Peltier G, Blanc G and Li-Beisson Y (2016) Lipidomic and transcriptomic analyses of *Chlamydomonas reinhardtii* under heat stress unveil a direct route for the conversion of membrane lipids into storage lipids. *Plant Cell Environ* **39**, 834–847.
  - 127 Kergomard J, Carrière F, Paboeuf G, Artzner F, Barouh N, Bourlieu C and Vié V (2022) Interfacial organization and phase behavior of mixed galactolipid-DPPC-phytosterol assemblies at the air-water interface and in hydrated mesophases. *Colloids Surf B Biointerfaces* **217**, 112646.
  - 128 Kessler F and Vidi P-A (2007) Plastoglobule lipid bodies: their functions in chloroplasts and their potential for applications. *Adv Biochem Eng Biotechnol* **107**, 153–172.
  - 129 Bréhélin C and Kessler F (2008) The plastoglobule: a bag full of lipid biochemistry tricks. *Photochem Photobiol* **84**, 1388–1394.
  - 130 Shivaiah K-K, Susanto FA, Devadasu E and Lundquist PK (2022) Plastoglobule lipid droplet isolation from plant leaf tissue and cyanobacteria. *J Vis Exp* doi: [10.3791/64515](https://doi.org/10.3791/64515)
  - 131 Choi YH, van Spronsen J, Dai Y, Verberne M, Hollmann F, Arends IWCE, Witkamp G-J and Verpoorte R (2011) Are natural deep eutectic solvents the missing link in understanding cellular metabolism and physiology? *Plant Physiol* **156**, 1701–1705.
  - 132 Durand E, Villeneuve P, Bourlieu-lacanal C and Carrière F (2021) Chapter six – natural deep eutectic solvents: hypothesis for their possible roles in cellular functions and interaction with membranes and other organized biological systems. In *Advances in Botanical Research* (Verpoorte R, Witkamp G-J and Choi YH, eds), pp. 133–158. Academic Press, Cambridge, MA.
  - 133 Dai Y, Varypataki EM, Golovina EA, Jiskoot W, Witkamp G-J, Choi YH and Verpoorte R (2021) Chapter seven – natural deep eutectic solvents in plants and plant cells: *in vitro* evidence for their possible functions. In *Advances in Botanical Research* (Verpoorte R, Witkamp G-J and Choi YH, eds), pp. 159–184. Academic Press, Cambridge, MA.
  - 134 Dai Y, Witkamp G-J, Verpoorte R and Choi YH (2013) Natural deep eutectic solvents as a new extraction media for phenolic metabolites in *Carthamus tinctorius* L. *Anal Chem* **85**, 6272–6278.
  - 135 González CG, Mustafa NR, Wilson EG, Verpoorte R and Choi YH (2018) Application of natural deep eutectic solvents for the “green” extraction of vanillin from vanilla pods. *Flavour Fragr J* **33**, 91–96.
  - 136 Ball S, Colleoni C, Cenci U, Raj JN and Tirtiaux C (2011) The evolution of glycogen and starch metabolism in eukaryotes gives molecular clues to understand the establishment of plastid endosymbiosis. *J Exp Bot* **62**, 1775–1801.
  - 137 Kroth PG, Chiovitti A, Gruber A, Martin-Jezequel V, Mock T, Parker MS, Stanley MS, Kaplan A, Caron L, Weber T *et al.* (2008) A model for carbohydrate metabolism in the diatom *Phaeodactylum tricornutum* deduced from comparative whole genome analysis. *PLoS One* **3**, e1426.
  - 138 Chabi M, Leleu M, Fermont L, Colpaert M, Colleoni C, Ball SG and Cenci U (2021) Retracing storage polysaccharide evolution in stramenopila. *Front Plant Sci* **12**, 629045.
  - 139 Tester RF, Karkalas J and Qi X (2004) Starch—composition, fine structure and architecture. *J Cereal Sci* **39**, 151–165.
  - 140 Goold H, Beisson F, Peltier G and Li-Beisson Y (2015) Microalgal lipid droplets: composition, diversity, biogenesis and functions. *Plant Cell Rep* **34**, 545–555.
  - 141 Li-Beisson Y, Kong F, Wang P, Lee Y and Kang B-H (2021) The disassembly of lipid droplets in *Chlamydomonas*. *New Phytol* **231**, 1359–1364.
  - 142 Moellering ER and Benning C (2010) RNA interference silencing of a major lipid droplet protein

- affects lipid droplet size in *Chlamydomonas reinhardtii*. *Eukaryot Cell* **9**, 97–106.
- 143 Nguyen HM, Baudet M, Cuiné S, Adriano J-M, Barthe D, Billon E, Bruley C, Beisson F, Peltier G, Ferro M *et al.* (2011) Proteomic profiling of oil bodies isolated from the unicellular green microalga *Chlamydomonas reinhardtii*: with focus on proteins involved in lipid metabolism. *Proteomics* **11**, 4266–4273.
  - 144 Ohlrogge J and Browse J (1995) Lipid biosynthesis. *Plant Cell* **7**, 957–970.
  - 145 Li X, Moellering ER, Liu B, Johnny C, Fedewa M, Sears BB, Kuo M-H and Benning C (2012) A galactoglycerolipid lipase is required for triacylglycerol accumulation and survival following nitrogen deprivation in *Chlamydomonas reinhardtii*. *Plant Cell* **24**, 4670–4686.
  - 146 Fan J, Andre C and Xu C (2011) A chloroplast pathway for the de novo biosynthesis of triacylglycerol in *Chlamydomonas reinhardtii*. *FEBS Lett* **585**, 1985–1991.
  - 147 Goodson C, Roth R, Wang ZT and Goodenough U (2011) Structural correlates of cytoplasmic and chloroplast lipid body synthesis in *Chlamydomonas reinhardtii* and stimulation of lipid body production with acetate boost. *Eukaryot Cell* **10**, 1592–1606.
  - 148 Bouillaud D, Heredia V, Castaing-Cordier T, Drouin D, Charrier B, Gonçalves O, Farjon J and Giraudeau P (2019) Benchtop flow NMR spectroscopy as an online device for the in vivo monitoring of lipid accumulation in microalgae. *Algal Res* **43**, 101624.
  - 149 Jaussaud A, Lupette J, Salvaing J, Jouhet J, Bastien O, Gromova M and Maréchal E (2020) Stepwise biogenesis of subpopulations of lipid droplets in nitrogen starved *Phaeodactylum tricornutum* cells. *Front. Plant Sci* **11**, 48.
  - 150 Kong F, Liang Y, Légeret B, Beyly-Adriano A, Blangy S, Haslam RP, Napier JA, Beisson F, Peltier G and Li-Beisson Y (2017) *Chlamydomonas* carries out fatty acid  $\beta$ -oxidation in ancestral peroxisomes using a bona fide acyl-CoA oxidase. *Plant J* **90**, 358–371.
  - 151 Selinski J and Scheibe R (2018) Malate valves: old shuttles with new perspectives. *Plant Biol (Stuttg)* **21**, 21–30.
  - 152 Lauersen KJ, Willamme R, Coosemans N, Joris M, Kruse O and Remacle C (2016) Peroxisomal microbodies are at the crossroads of acetate assimilation in the green microalga *Chlamydomonas reinhardtii*. *Algal Res* **16**, 266–274.
  - 153 Calatrava V, Tejada-Jimenez M, Sanz-Luque E, Fernandez E and Galvan A (2023) Chapter 3 – nitrogen metabolism in *Chlamydomonas*. In *The Chlamydomonas Sourcebook* (Grossman AR and Wollman F-A, eds), 3rd, 3rd edn, pp. 99–128. Academic Press, London.
  - 154 Huang W, Krishnan A, Plett A, Meagher M, Linka N, Wang Y, Ren B, Findinier J, Redekop P, Fakhimi N *et al.* (2023) *Chlamydomonas* mutants lacking chloroplast triose phosphate Transporter3 are metabolically compromised and light sensitive. *Plant Cell* **35**, 2592–2614.
  - 155 Bailleul B, Berne N, Murik O, Petroutsos D, Prihoda J, Tanaka A, Villanova V, Bligny R, Flori S, Falconet D *et al.* (2015) Energetic coupling between plastids and mitochondria drives CO<sub>2</sub> assimilation in diatoms. *Nature* **524**, 366–369.
  - 156 Wu C, Xiong W, Dai J and Wu Q (2015) Genome-based metabolic mapping and <sup>13</sup>C flux analysis reveal systematic properties of an oleaginous microalga *Chlorella protothecoides*. *Plant Physiol* **167**, 586–599.
  - 157 Singh H, Shukla MR, Chary KVR and Rao BJ (2014) Acetate and bicarbonate assimilation and metabolite formation in *Chlamydomonas reinhardtii*: a <sup>13</sup>C-NMR study. *PLoS One* **9**, e106457.
  - 158 Zhou B, Xiao JF, Tuli L and Ressom HW (2012) LC-MS-based metabolomics. *Mol Biosyst* **8**, 470–481.
  - 159 Wishart DS, Cheng LL, Copié V, Edison AS, Eghbalian HR, Hoch JC, Gouveia GJ, Pathmasiri W, Powers R, Schock TB *et al.* (2022) NMR and metabolomics—a roadmap for the future. *Metabolites* **12**, 678.
  - 160 Edison AS, Colonna M, Gouveia GJ, Holderman NR, Judge MT, Shen X and Zhang S (2021) NMR: unique strengths that enhance modern metabolomics research. *Anal Chem* **93**, 478–499.
  - 161 Alshamleh I, Krause N, Richter C, Kurrle N, Serve H, Günther UL and Schwalbe H (2020) Real-time NMR spectroscopy for studying metabolism. *Angew Chem Int Ed* **59**, 2304–2308.
  - 162 Judge MT, Wu Y, Tayyari F, Hattori A, Glushka J, Ito T, Arnold J and Edison AS (2019) Continuous in vivo metabolism by NMR. *Front Mol Biosci* **6**, 26.
  - 163 Cerofolini L, Giuntini S, Barbieri L, Pennestri M, Codina A, Fragai M, Banci L, Luchinat E and Ravera E (2019) Real-time insights into biological events: in-cell processes and protein-ligand interactions. *Biophys J* **116**, 239–247.
  - 164 Thiam AR, Farese RV Jr and Walther TC (2013) The biophysics and cell biology of lipid droplets. *Nat Rev Mol Cell Biol* **14**, 775–786.
  - 165 McFearn CL, Beaman DK, Moore FG and Richmond GL (2009) From Franklin to today: toward a molecular level understanding of bonding and adsorption at the oil–water interface. *J Phys Chem C* **113**, 1171–1188.
  - 166 Ruiz-Lopez MF, Francisco JS, Martins-Costa MTC and Anglada JM (2020) Molecular reactions at aqueous interfaces. *Nat Rev Chem* **4**, 459–475.
  - 167 Li G and Zuo YY (2022) Molecular and colloidal self-assembly at the oil–water interface. *Curr Opin Colloid Interface Sci* **62**, 101639.

- 168 Verger R and de Haas G (1976) Interfacial enzyme kinetics of lipolysis. *Annu Rev Biophys Bioeng* **5**, 77–117.
- 169 Bénarouche A, Habchi J, Cagna A, Maniti O, Girard-Egrot A, Cavalier J-F, Longhi S and Carrière F (2017) Interfacial properties of NTAIL, an intrinsically disordered protein. *Biophys J* **113**, 2723–2735.
- 170 Baldwin PM (2001) Starch granule-associated proteins and polypeptides: a review. *Starke* **53**, 475–503.
- 171 Findinier J, Laurent S, Duchêne T, Roussel X, Lancelon-Pin C, Cuiné S, Putaux J-L, Li-Beisson Y, D'Hulst C, Wattedled F *et al.* (2019) Deletion of BSG1 in *Chlamydomonas reinhardtii* leads to abnormal starch granule size and morphology. *Sci Rep* **9**, 1990.
- 172 Itakura AK, Chan KX, Atkinson N, Pallesen L, Wang L, Reeves G, Patena W, Caspari O, Roth R, Goodenough U *et al.* (2019) A RuBisCO-binding protein is required for normal pyrenoid number and starch sheath morphology in *Chlamydomonas reinhardtii*. *Proc Natl Acad Sci USA* **116**, 18445–18454.
- 173 Gromova M, Guillermo A, Bayle P-A and Bardet M (2015) *In vivo* measurement of the size of oil bodies in plant seeds using a simple and robust pulsed field gradient NMR method. *Eur Biophys J* **44**, 121–129.
- 174 Møller BL and Laursen T (2021) Chapter eight – metabolons and bio-condensates: the essence of plant plasticity and the key elements in development of green production systems. In *Advances in Botanical Research* (Verpoorte R, Witkamp G-J and Choi YH, eds), pp. 185–223. Academic Press, Cambridge, MA.
- 175 Minton AP (2001) The influence of macromolecular crowding and macromolecular confinement on biochemical reactions in physiological media. *J Biol Chem* **276**, 10577–10580.
- 176 Ellis RJ and Minton AP (2003) Join the crowd. *Nature* **425**, 27–28.
- 177 Shahid S, Hassan MI, Islam A and Ahmad F (2017) Size-dependent studies of macromolecular crowding on the thermodynamic stability, structure and functional activity of proteins: *in vitro* and *in silico* approaches. *Biochim Biophys Acta Gen Subj* **1861**, 178–197.
- 178 Ahmed MC, Crehuet R and Lindorff-Larsen K (2020) Computing, analyzing, and comparing the radius of gyration and hydrodynamic radius in conformational ensembles of intrinsically disordered proteins. *Methods Mol Biol* **2141**, 429–445.
- 179 Fonin AV, Darling AL, Kuznetsova IM, Turoverov KK and Uversky VN (2018) Intrinsically disordered proteins in crowded milieu: when chaos prevails within the cellular gumbo. *Cell Mol Life Sci* **75**, 3907–3929.
- 180 Cedeño C, Pauwels K and Tompa P (2017) Protein delivery into plant cells: toward *in vivo* structural biology. *Front Plant Sci* **8**, 519.
- 181 Böhm J (1857) Beiträge zur näheren kenntnis des chlorophylls. *Gerold [in Komm]*.
- 182 Mohl HV (1855) Über den bau des chlorophylls. *Bot Ztg* **13**, 105.
- 183 Yewdall NA, André AAM, Lu T and Spruijt E (2021) Coacervates as models of membraneless organelles. *Curr Opin Colloid Interface Sci* **52**, 101416.
- 184 Oparin AI (1957) The Origin of Life on the Earth. 3rd edn. Oliver & Boyd, Edinburgh; London.
- 185 Ghosh B, Bose R and Tang T-YD (2021) Can coacervation unify disparate hypotheses in the origin of cellular life? *Curr Opin Colloid Interface Sci* **52**, 101415.
- 186 Bonucci A, Ouari O, Guigliarelli B, Belle V and Mileo E (2020) *In-cell* EPR: progress towards structural studies inside cells. *ChemBiochem* **21**, 451–460.
- 187 Zurn P, Bassett DS and Rust NC (2020) The citation diversity statement: a practice of transparency, a way of life. *Trends Cogn Sci* **24**, 669–672.
- 188 Anderson LE and Carol AA (2004) Enzyme co-localization with RuBisCO in pea leaf chloroplasts. *Photosynth res* **82**, 49–58.
- 189 Sainis JK and Harris GC (1986) The association of ribulose-1,5-bisphosphate carboxylase with phosphoriboisomerase and phosphoribulokinase. *Biochem Biophys res Commun* **139**, 947–954.
- 190 Anderson LE, Goldhaber-Gordon IM, Li D, Tang XY, Xiang M and Prakash N (1995) Enzyme-enzyme interaction in the chloroplast: glyceraldehyde-3-phosphate dehydrogenase, triose phosphate isomerase and aldolase. *Planta* **196**, 245–255.
- 191 Dani DN and Sainis JK (2005) Isolation and characterization of a thylakoid membrane module showing partial light and dark reactions. *Biochim Biophys Acta* **1669**, 43–52.
- 192 Persson LO and Johansson G (1989) Studies of protein-protein interaction using countercurrent distribution in aqueous two-phase systems. Partition behaviour of six Calvin-cycle enzymes from a crude spinach (*Spinacia oleracea*) chloroplast extract. *Biochem J* **259**, 863–870.
- 193 Süß K-H, Prokhorenko I and Adler K (1995) *In situ* association of Calvin cycle enzymes, ribulose-1,5-bisphosphate carboxylase/oxygenase activase, ferredoxin-NADP<sup>+</sup> reductase, and nitrite reductase with thylakoid and pyrenoid membranes of *Chlamydomonas reinhardtii* chloroplasts as revealed by immunoelectron microscopy. *Plant Physiol* **107**, 1387–1397.
- 194 Scheibe R, Wedel N, Vetter S, Emmerlich V and Sauermann S-M (2002) Co-existence of two regulatory NADP-glyceraldehyde 3-P dehydrogenase complexes in higher plant chloroplasts. *Eur J Biochem* **269**, 5617–5624.
- 195 Wedel N, Soll J and Paap BK (1997) CP12 provides a new mode of light regulation of Calvin cycle activity in higher plants. *Proc Natl Acad Sci USA* **94**, 10479–10484.

- 196 Marri L, Trost P, Pupillo P and Sparla F (2005) Reconstitution and properties of the recombinant glyceraldehyde-3-phosphate dehydrogenase/CP12/phosphoribulokinase supramolecular complex of *Arabidopsis*. *Plant Physiol* **139**, 1433–1443.
- 197 Oesterhelt C, Klocke S, Holtgreffe S, Linke V, Weber APM and Scheibe R (2007) Redox regulation of chloroplast enzymes in *Galdieria sulphuraria* in view of eukaryotic evolution. *Plant Cell Physiol* **48**, 1359–1373.
- 198 Blanc-Garin V, Veaudor T, Sétif P, Gontero B, Lemaire SD, Chauvat F and Cassier-Chauvat C (2022) First in vivo analysis of the regulatory protein CP12 of the model cyanobacterium *Synechocystis* PCC 6803: biotechnological implications. *Front Plant Sci* **13**, 999672.
- 199 Wedel N and Soll J (1998) Evolutionary conserved light regulation of Calvin cycle activity by NADPH-mediated reversible phosphoribulokinase/CP12/glyceraldehyde-3-phosphate dehydrogenase complex dissociation. *Proc Natl Acad Sci USA* **95**, 9699–9704.
- 200 Tamoi M, Miyazaki T, Fukamizo T and Shigeoka S (2005) The Calvin cycle in cyanobacteria is regulated by CP12 via the NAD(H)/NADP(H) ratio under light/dark conditions. *Plant J* **42**, 504–513.
- 201 Avilan L, Gontero B, Lebreton S and Ricard J (1997) Memory and imprinting effects in multienzyme complexes. *Eur J Biochem* **246**, 78–84.
- 202 Graciet E, Lebreton S, Camadro J-M and Gontero B (2003) Characterization of native and recombinant A4 glyceraldehyde 3-phosphate dehydrogenase. Kinetic evidence for conformation changes upon association with the small protein CP12. *Eur J Biochem* **270**, 129–136.
- 203 Mekhalfi M, Puppo C, Avilan L, Lebrun R, Mansuelle P, Maberly SC and Gontero B (2014) Glyceraldehyde-3-phosphate dehydrogenase is regulated by ferredoxin-NADP reductase in the diatom *Asterionella formosa*. *New Phytol* **203**, 414–423.
- 204 Launay H, Barré P, Puppo C, Manneville S, Gontero B and Receveur-Bréchet V (2016) Absence of residual structure in the intrinsically disordered regulatory protein CP12 in its reduced state. *Biochem Biophys Res Commun* **477**, 20–26.
- 205 Launay H, Barré P, Puppo C, Zhang Y, Manneville S, Gontero B and Receveur-Bréchet V (2018) Cryptic disorder out of disorder: encounter between conditionally disordered CP12 and glyceraldehyde-3-phosphate dehydrogenase. *J Mol Biol* **430**, 1218–1234.